

Proceedings of the Royal society of London (B)
(Biological sciences)

November 2013, Volume 280 (1770), Pages 2013.1876

<http://dx.doi.org/10.1098/rspb.2013.1876>

© 2013 The Author(s) Published by the Royal Society. All rights reserved

Archimer
<http://archimer.ifremer.fr>

Cryptic species of *Archinome* (Annelida: Amphinomida) from vents and seeps

Elizabeth Borda^{1,9,*}, Jerry D. Kudenov², Pierre Chevaldonné³, James A. Blake⁴, Daniel Desbruyères⁶, Marie-Claire Fabri⁶, Stéphane Hourdez⁷, Fredrik Pleijel⁸, Timothy M. Shank⁵, Nerida G. Wilson¹, Anja Schulze⁹ and Greg W. Rouse^{1,*}

¹ Scripps Institution of Oceanography, UC San Diego, La Jolla, CA 93093, USA

² Department of Biological Sciences, University of Alaska Anchorage, Anchorage, AK 99508, USA

³ CNRS, UMR 7263 IMBE, Institut Méditerranéen de la Biodiversité et d'Ecologie Marine et Continentale, Aix-Marseille Université, Station Marine d'Endoume, Rue de la Batterie des Lions, 13007 Marseille, France

⁴ AECOM Marine and Coastal Center, Woods Hole, MA 02543, USA

⁵ Woods Hole Oceanographic Institution, Woods Hole, MA 02543, USA

⁶ Département Etude des Ecosystèmes Profonds, Centre de Brest de l'IFREMER, 29280 Plouzané Cedex, France

⁷ CNRS, UPMC UMR 7127, Station Biologique de Roscoff, 29682 Roscoff, France

⁸ Department of Marine Ecology, University of Gothenburg, Tjärnö, Strömstad, Sweden

⁹ Marine Biology Department, Texas A&M University at Galveston, Galveston, TX 77553, USA

*: Corresponding authors : Elisabeth Borda, email address : lizborda@gmail.com ; Greg W. Rouse, email address : grouse@ucsd.edu

Abstract:

Since its description from the Galapagos Rift in the mid-1980s, *Archinome rosacea* has been recorded at hydrothermal vents in the Pacific, Atlantic and Indian Oceans. Only recently was a second species described from the Pacific Antarctic Ridge. We inferred the identities and evolutionary relationships of *Archinome* representatives sampled from across the hydrothermal vent range of the genus, which is now extended to cold methane seeps. Species delimitation using mitochondrial cytochrome c oxidase subunit I (COI) recovered up to six lineages, whereas concatenated datasets (COI, 16S, 28S and ITS1) supported only four or five of these as clades. Morphological approaches alone were inconclusive to verify the identities of species owing to the lack of discrete diagnostic characters. We recognize five *Archinome* species, with three that are new to science. The new species, designated based on molecular evidence alone, include: *Archinome levinae* n. sp., which occurs at both vents and seeps in the east Pacific, *Archinome tethyana* n. sp., which inhabits Atlantic vents and *Archinome jasoni* n. sp., also present in the Atlantic, and whose distribution extends to the Indian and southwest Pacific Oceans. Biogeographic connections between vents and seeps are highlighted, as are potential evolutionary links among populations from vent fields located in the east Pacific and Atlantic Oceans, and Atlantic and Indian Oceans; the latter presented for the first time.

Keywords: deep sea ; hydrothermal vents ; cold methane seeps ; cryptic species ; polychaete

Introduction

It has been more than three decades since the discovery of deep ocean chemosynthetic communities. Over 600 animal species have been described from these habitats, mainly from hydrothermal vents near active tectonic plate boundaries, as well as from hydrocarbon seeps along continental margins [1–3]. Biodiversity patterns among deep-sea chemosynthetic fauna have been discussed at length in the context of taxonomic and environmental affinities leading to the designation of various biogeographic 'provinces' [1,3–6]. The few rigorous studies that have inferred these patterns in a phylogenetic context and on a broad scale [7–11] have focused on Pacific Ocean taxa [8,12–15]. Deep ocean currents, plate tectonics, seafloor spreading rates, oxygen levels, bathymetry, larval dispersal capabilities and sulfide or methane-rich communities, such as sunken wood and whale falls, as potential evolutionary 'stepping stones', are just some of the extrinsic factors that have been posited to drive species distributions in deep ocean chemosynthetic habitats [1,15–17].

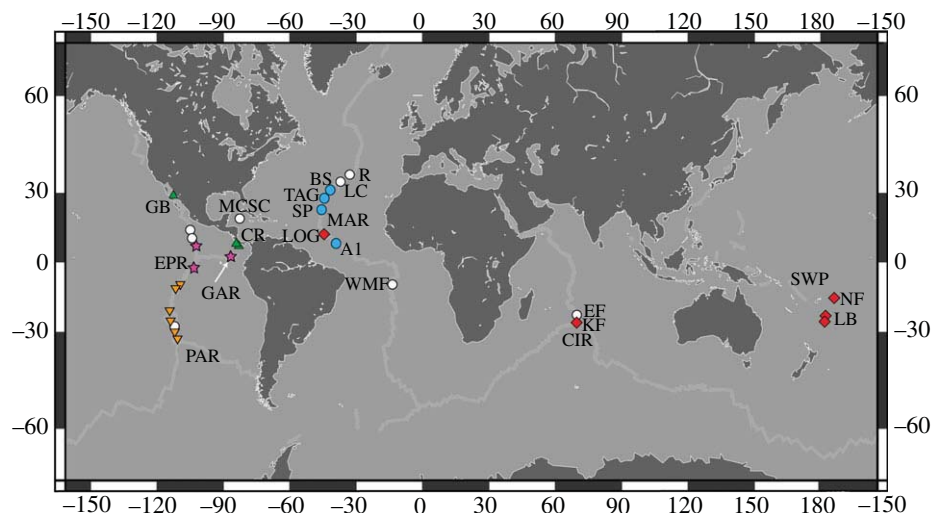


Figure 1. Distribution map of *Archinome* species. Symbols indicate all known records, with sites sampled for this study denoted by triangles (*A. levinae* n. sp.), stars (*A. rosacea*), inverted triangles (*A. storchi*), circles (*A. tethyana* n. sp.), diamonds (*A. jasoni* n. sp.) and open circles (unsampled records). A1, Ashadze-1; BS, Broken Spur; CIR, Central Indian Ridge; CRM, Costa Rica Margin; EF, Edmund Field; EPR, East Pacific Rise; GAR, Galapagos Rift; GB, Guaymas Basin; KF, Kairei Field; LOG, Logatchev; LB, Lau Basins (KLM and TML); LC, Lost City; MAR, Mid-Atlantic Ridge; MCSC, Mid-Cayman Spreading Center; PAR, Pacific Antarctic Ridge; R, Rainbow; SP, Snake Pit; SWP, southwest Pacific basins; TAG, TAG; WMF, Wideawake Mussel Field. (Online version in colour.)

Significant effort has been put forth in characterizing the faunal communities of these dynamic ecosystems. Traditional taxonomy, which emphasizes the characterization of morphological diversity, cannot always account for other biological attributes, such as developmental [18] and ecological adaptations [7,19,20], leading to over or underestimates of diversity [17,21]. Molecular systematics has been a useful tool to provide a testable framework to infer evolutionary relationships of genetic lineages, independent of phenotypic, ontogenetic and ecological variation. The integration of molecular data has greatly improved our knowledge of species delimitations and distributions, however with the caveat that taxonomic, genetic and geographical diversity estimates are all sensitive to sampling [22].

Annelids account for approximately 20% (approx. 111 species) of the named hydrothermal vent animal species [2]. The East Pacific Rise (EPR) has among the best-studied vent annelids [23–30] and the incorporation of molecular data has shed light on cryptic diversity found along this system [12,14,21,31,32]. The giant vestimentiferan tubeworm, *Riftia pachyptila*, is a dominant feature of hydrothermal vent sites along the EPR and was shown to be genetically homogeneous across a broad range (27° N–32° S), with a genetic break identified at the Easter microplate (approx. 26° S) [14]. The thermally tolerant *Alvinella pompejana* is known only from the EPR and although morphologically similar across a distance of approximately 5000 km (21° N–32° S), mitochondrial (mt) data revealed a north/south genetic break [14,33]. Species of *Alvinella* and *Riftia* are restricted to the east Pacific, whereas *Paralvinella* is amphi-Pacific, though so far not recorded outside of this ocean [2,34]. Major annelid clades are represented on a broad geographical scale throughout diverse chemosynthetic environments (e.g. Siboglinidae and Polynoidae), but among vent animals, only two ‘species’ have been recorded on a global scale: the ampharetid *Amphisamytha galapagensis* [8,35] and the amphinomid *Archinome rosacea* [36,37]; the latter being the focus of this study, while the former is now known to be a species complex [8].

Amphinomids are best represented by the stinging fireworms (e.g. *Eurythoe* and *Hermodice*), which are common inhabitants of tropical reef environments [38,39]. *Archinome rosacea* was the first amphinomid described from chemosynthetic habitats from the original 1979 collections from *Rose Garden*, located at the Galapagos Rift (GAR; 0° N; 2400 m) in the eastern Pacific [36]. Since its description in 1985, *Archinome* has been recorded across major spreading centres in the Pacific, Atlantic and Indian Oceans (figure 1) [2,40]. *Archinome* specimens (figure 2 and electronic supplementary material, figure S1) are easily recognizable among vent fauna, with prominent calcareous, bifurcate (forked) chaetae, an elongate trilobed caruncle (figure 2*b,c*), a fusiform (spindle-like) body shape, prominent mid-ventral muscular scutes (figure 2*g*) and can range in size from just a few millimetres to several centimetres. In 2006, the distribution of *A. rosacea* was restricted to the GAR and the northeast Pacific Rise (NEPR) [2], in contrast to earlier accounts, which proposed a more widespread range including the Guaymas Basin (GB) sedimented vents, Mid-Atlantic Ridge (MAR) and Central Indian Ridge (CIR) vent systems [41,42]. Referencing unpublished data, Desbruyères *et al.* [2] suggested the presence of at least three additional species, yet until recently *A. rosacea* remained the only named species. In 2009, *Archinome storchi* [40] was described from the Pacific Antarctic Ridge (PAR, 37° S). Also until recently, *Archinome* had only been recorded from hydrothermal vents. In 2009 and 2010, specimens were collected from cold methane seeps located at the Costa Rica margin (CRM) [43]. *Archinome* has been collected from a broad range of vent localities (figure 1) and depths (1000–3500 m) [40], however it is now known to occur at depths greater than 4000 m, including Ashadze-1 (A1; 12° N, MAR; 4080 m) [44].

Given *Archinome*'s broad distribution and uncertainty as to the number of species within the genus, we used an integrative systematic approach to: (i) infer the identities of *Archinome* specimens from across the ‘cosmopolitan’ range among vent systems; (ii) infer the evolutionary relationships among vent and seep *Archinome* and (iii) and explore the biogeographic links and diversification patterns across the Atlantic, Indian and Pacific Oceans.

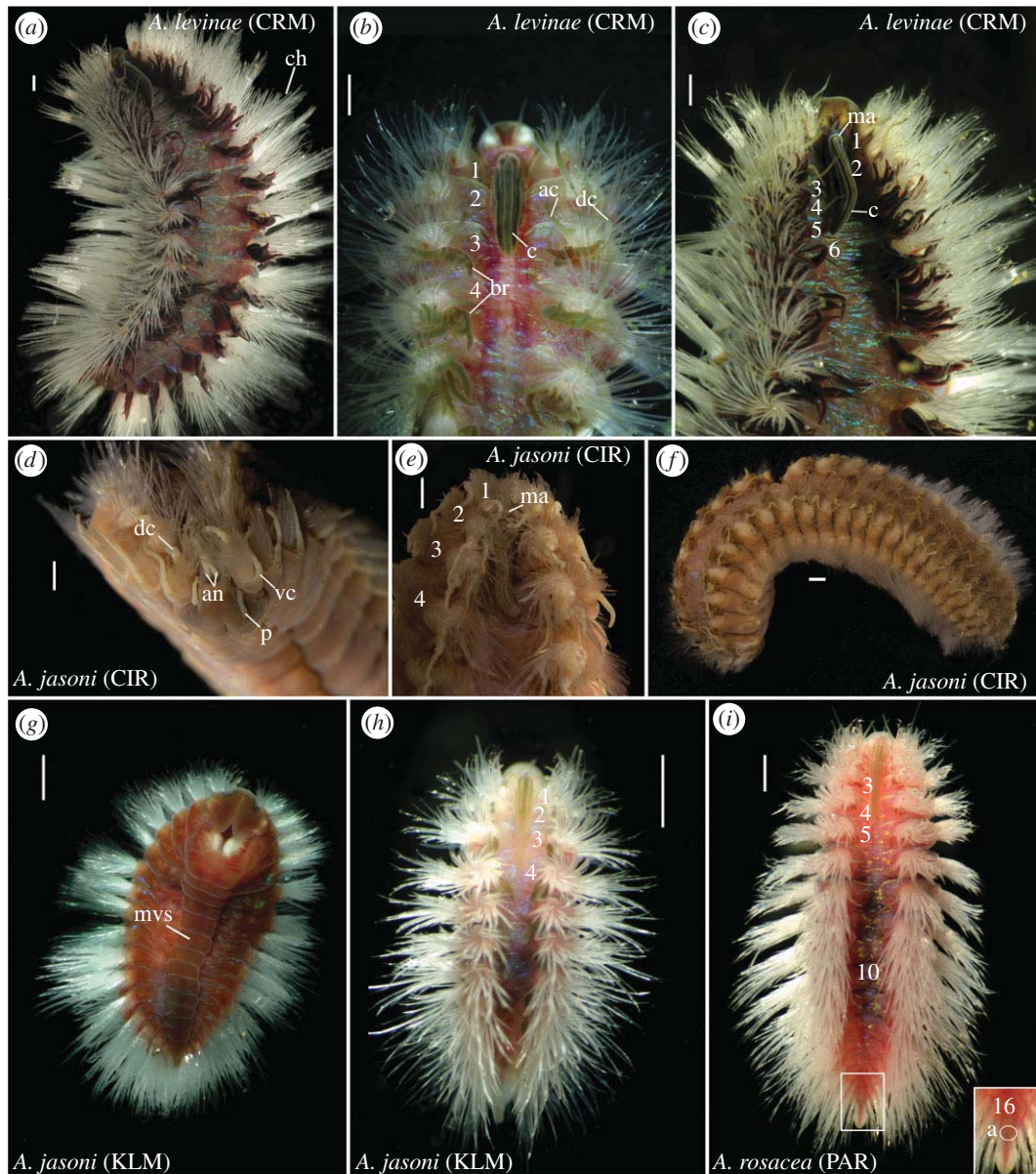


Figure 2. *Archinome* species. (a) (Live) whole body, dorsal view of *A. levinae* n. sp. (purple morph; SIO-BIC AXXXX); (b) (Live) Dorsal view of anterior body segments Q6 of *A. levinae* n. sp. (SIO-BIC A1398; CRM, 9° N); (c) (Live) Dorsal view of anterior body segments of *A. levinae* n. sp. (purple morph; SIO-BIC AXXXX); (d) (Preserved) Frontal view of *A. jasoni* n. sp. (SIO-BIC A2313; CIR); (e) (Preserved) Dorsal view of anterior body segments of *A. jasoni* n. sp. (SIO-BIC A2313); (f) (Preserved) Whole body, dorso-lateral view of *A. jasoni* n. sp. (SIO-BIC A2313); (g) (Live) Whole body, ventral view of *A. jasoni* n. sp. (KML); (h) (Live) Whole body, dorsal view of *A. jasoni* n. sp. (KML); (i) (Live) Dorsal view of *A. storchi* (PAR). Note within species variation in caruncle length and size for *A. levinae* n. sp. and *A. jasoni* n. sp. Scale bars, 1 mm. a, anus; an, antennae; ac, accessory dorsal cirrus; br, branchia; c, caruncle; ch, chaetae; dc, dorsal cirrus; ma, median antenna; mvs, mid-ventral scutes; vc, ventral cirrus; numbers denote segments. (Online version in colour.)

Q7

2. Material and methods

(a) Sample collection

Archinome samples were collected using remotely operated vehicles including Woods Hole Oceanographic Institution's (WHOI) *Jason I* (R/V *Knorr*) and *Jason II* (R/V *Melville*), Monterey Bay Aquarium Research Institute's *Tiburon* (R/V *Western Flyer*) and Institut Français de Recherche pour l'Exploitation de la Mer's (IFREMER) *Victor 6000* (R/V *Pourquoi Pas?*), and human occupied vehicles *Alvin* (WHOI) and *Nautile* (IFREMER) during deep-sea expeditions between 1990 through 2010. Figure 1 shows known records and sampling localities from vent and seep communities included in this study. Specimens were sampled from among larger vent fauna such as Vestimentifera and mytilid bivalves, as well as from upper sediment layer samples obtained from suction samplers and mesh scoops. Specimens were sorted aboard research vessels and when possible relaxed in a 50:50 (7% MgCl₂: seawater) MgCl₂ solution,

followed by preservation in 10% formalin, then transferred to 70% ethanol for morphological evaluation and 80–95% Ethanol or stored at -80°C for molecular work. Molecular samples were kept cold at 4°C or frozen at -80°C or -20°C . Collection and voucher information and details regarding evaluation of morphology can be found in the electronic supplementary material, text and tables S1, S4 and S5).

(b) Gene data collection, phylogenetic methods and genetic structure

Protocols for whole genomic DNA extraction, amplification and sequencing procedures are as reported by Borda *et al.* [45], unless stated otherwise. Electronic supplementary material, table S2 lists primers and annealing temperature profiles used for amplification of mt cytochrome c oxidase subunit I (COI), and mt 16S rDNA (16S). Amplification protocols for the nuclear internal transcribed spacer 1 (ITS1) and 28S rDNA (28S) followed Nygren &

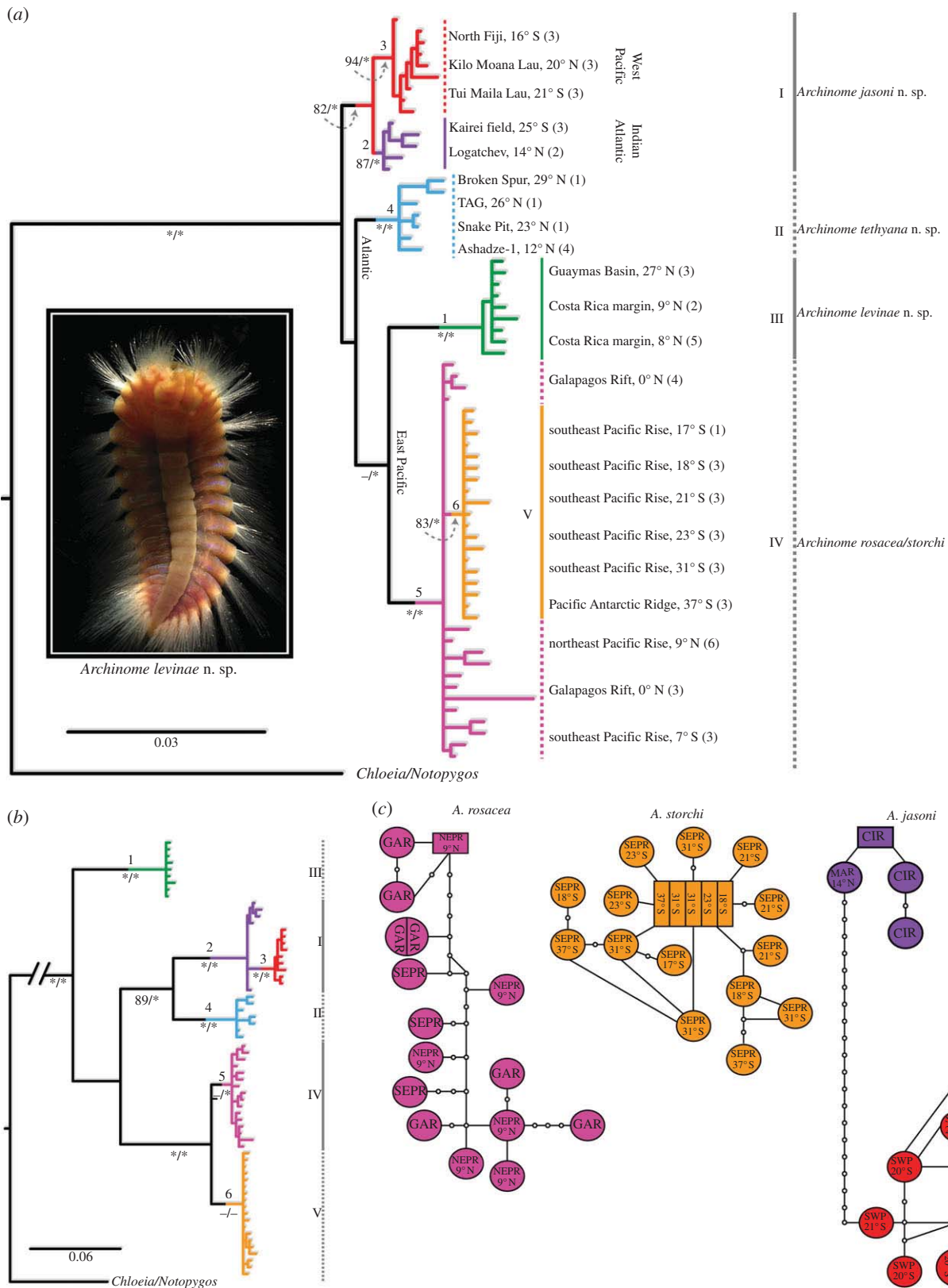


Figure 3. Phylogeny (BI topology shown) and genetic diversity of *Archinome* species. (a) $COI_{no3rd} + 16S + 28S + ITS1$; (b) $COI_{all} + 16S + 28S + ITS1$. Roman numerals specify species clades; numerals 1–6 (above nodes) correspond to clades recovered in (b); ML bootstrap and BI posterior probabilities (boot/pp) shown below nodes; asterisk (*) denotes boot > 90% and pp > 0.95; values below 80% denoted by minus sign '-'. (c) $COI_{all} + 16S$ statistical parsimony haplotype networks (fixed 21-step connection limit) for *A. rosacea*, *A. storchi* and *A. jasoni* n. sp. Coloured circles and rectangles are scaled to size according to number of individuals per haplotype. Two or more names indicate identical shared haplotypes. Small open circles represent unsampled haplotypes. (Online version in colour.)

Pleijel [46] and Borda *et al.* [45], respectively. All data were analysed using maximum-likelihood (ML) and Bayesian inference (BI) procedures following methods described in [45], as was the choice of outgroup to root the analyses (i.e. *Chloelia viridis*). *Notopygos ornata* was included as an additional outgroup taxon based on hypothesized affinities based on body shape and

branchial morphology [37,45]. Phylogenetic trees (figure 3) are based on the BI topology, unless stated otherwise (see electronic supplementary material, figures S3 and S4), with support values (i.e. ML bootstrap (boot); posterior probabilities (pp)) indicated at nodes. Haplotype networks were generated for combined $COI + 16S$ using TCS v. 1.21 [47], based on maximum parsimony

Table 1. *Archinome* pairwise distances. Mean Timura Nei (TrN; below diagonal) and uncorrected (above diagonal) interclade and intraclade (TrN; italics along diagonal) pairwise distances for COI and ITS1 (bold).

	I	II	III	IV	V
I. <i>Archinome jasoni</i> n. sp.	0.017 0.001	0.106 0.013	0.133 0.020	0.144 0.013	0.139 0.013
II. <i>Archinome tethyana</i> n. sp.	0.118 0.014	0.009 0.000	0.130 0.032	0.112 0.025	0.112 0.025
III. <i>Archinome levinae</i> n. sp.	0.150 0.020	0.145 0.033	0.004 0.000	0.125 0.031	0.130 0.032
IV. <i>Archinome rosacea</i>	0.168 0.013	0.124 0.025	0.140 0.032	0.006 0.004	0.047 0.004
V. <i>A. storchi</i>	0.161 0.014	0.125 0.026	0.147 0.033	0.049 0.004	0.003 0.000

and with a 95% probability (14-step connection limit) and fixed step connection limits ranging 10–50; gaps were treated as missing data. GenBank (16S, COI: JX027992–JX028115; 28S: JX028121–JX028141; ITS: KF288935–KF288959) and voucher accession numbers are provided in the electronic supplementary material, table S1. See also the electronic supplementary material, text for extended phylogenetic methods and sequence evaluation criteria.

3. Results

We inferred the phylogenetic relationships of *Archinome* specimens from COI (59 sequences; approx. 654 bp), 16S (65 sequences; approx. 472 bp), 28S (21 sequences; approx. 966 bp) and ITS1 (25 sequences; 572 bp). Table 1 provides mean intraclade and interclade TrN corrected and uncorrected pairwise distances for complete COI (d_{COI}) and ITS1 (d_{ITS}). COI exhibited the highest genetic divergences among clade terminals with the majority of synonymous changes occurring in third codon positions. COI saturation plots (see electronic supplementary material, figure S2) indicated that third position transitions reached saturation after approximately 13% sequence divergence. First and second codon position transitions and first through third codon position transversions were not saturated (results not shown). Interclade relationships and species identification were evaluated with the inclusion (COI_{ALL}) and exclusion (COI_{no3rd}) of COI third codon positions in combined analyses with 16S, 28S and ITS1 (figure 3). Results from individual and mt gene analyses can be found in the electronic supplementary material, figures S3 and S4. Mean COI interclade-corrected genetic distances were 12.5%, ranging 2.7–18.3%, and mean intraclade-corrected genetic distances was 0.5%, ranging 0–1.1%. ITS1 exhibited low divergences in comparison to COI. The highest corrected genetic pairwise distance was 3.6%. Mean ITS1 interclade-corrected genetic distance was 1.8%, ranging 1.0–3.6%, and mean intraclade-corrected genetic distance was 0.1%, ranging 0–1.0% (see table 1 and electronic supplementary material, table S3). Refer to the electronic supplementary material, text for results regarding morphological evaluation.

The phylogenetic relationships among *Archinome* species accepted here are based on COI_{no3rd} + 16S + 28S + ITS

(figure 3a). The data supported four *Archinome* clades, I–IV, of which three are regarded as new species and described in the electronic supplementary material, text. Numerical clades 1–6 above nodes correspond to those recovered in the analyses of concatenated COI_{ALL} + 16S + 28S + ITS1 (figure 3b; see also the electronic supplementary material, figure S3A). Clade I (boot/pp = 82/0.94; d_{COI} = 1.7%), hereafter *Archinome jasoni* n. sp., included the southwest (SW) Pacific vent specimens (clade 3; boot/pp = 94/1.0; d_{COI} = 0.5%) from North Fiji (NF; 16° S; 1985 m), Kilo Moana Lau (KML; 20° S; 2650 m) and Tui Malila Lau (TML; 21° S; 1900 m) and clade 2 (boot/pp = 87/1.0; d_{COI} = 0.3%), which included specimens from Logatchev (14° N, MAR, 3038 m) and Kairei field (25° S, CIR, 2432 m). *Archinome jasoni* n. sp. was supported as sister to the remaining *Archinome* species (boot/pp = 100/0.98). The highest *A. jasoni* n. sp. d_{COI} was 3.6% between specimens from NF/KML and LOG. The lowest interclade d_{COI} was 10.4% (CIR, clade 2) with clade II (boot/pp = 100/1.0); hereafter, *Archinome tethyana* n. sp. The *A. tethyana* n. sp. clade included the northern MAR specimens (clade 4; boot/pp = 99/1.0). Sequence data for all four genes were available for A1 (MAR) specimens; only three representative 16S sequences (see electronic supplementary material, figure S3B) were available from Broken Spur (29° N; 3056 m), TAG (26° N; 3655 m) and Snake Pit (23° N; 3660 m). Clade III (clade 1; boot/pp = 98/1.0; mean d_{COI} = 0.4%), hereafter, *Archinome levinae* n. sp., included specimens from GB vents (27° N; approx. 2400 m) and CRM seeps (8–9° N; 1000–1800 m). The highest *A. levinae* n. sp. d_{COI} was 0.9% and the lowest interclade d_{COI} was 13.2% (with clade IV). *Archinome levinae* n. sp. was sister to Clade IV (boot/pp = 98/1.0; d_{COI} = 2.7%), representing *A. rosacea* and *A. storchi* (Clade V) from the GAR, EPR and PAR (clades 5 and 6; figure 3b). Clade 5 (d_{COI} = 0.6%) included *A. rosacea* from GAR, as well as specimens from EPR 9° N (2500 m) and 7° S (2700 m). Clade 6 (d_{COI} = 0.3%; boot/pp = 83/1.0) was comprised PAR specimens and those sampled northward along the southeast Pacific Rise (SEPR) from 31° S to 17° S (2200–2500 m). Clade 6 was a subclade nested among unresolved *A. rosacea* representatives (see also the electronic supplementary material, figures S3B and S4A). The highest d_{COI} was 5.7%, between representatives from the

GAR (*A. rosacea*) and 17° S (*A. storchi*). The lowest interclade d_{COI} was 11.9%, between *A. tethyana* n. sp. and *A. rosacea* (9° N, 7° S). The positions of *A. tethyana* n. sp. and *A. levinae* n. sp. received low (boot/pp = 52/0.78) to moderate support (boot/pp = 74/1.0), respectively.

Evaluation of concatenated $\text{COI}_{\text{ALL}} + 16\text{S} + 28\text{S} + \text{ITS1}$ (figure 3b) supported that *Archinome* was comprised five clades showing minimal geographical overlap. The resulting topology was similar to that of COI_{ALL} (see electronic supplementary material, figures S3A and S2B), with the exception that *A. jasoni* n. sp. clade 3 was nested within clade 2, instead of showing reciprocal monophyly (figure 3a). The topology deviated from that observed in figure 3a, in that vent/seep *A. levinae* n. sp. was the sister group to the remaining *Archinome* species and reciprocally monophyletic (boot/pp = 95/1.0). *A. rosacea* (boot/pp = 77/0.66) and *A. storchi* (boot/pp = 75/1.0) clades were recovered; each clade with low support, however. Combined $\text{COI}_{\text{ALL}} + 16\text{S}$ data ($n = 35$) supported distinct networks (even with a fixed 50 step connection limit) for *A. rosacea* ($n = 16$) and *A. storchi* ($n = 19$), each containing 15 haplotypes. A single haplotype was shared between two *A. rosacea* individuals (GAR), while one haplotype was shared among five *A. storchi* individuals from the SEPR (figure 3c). No haplotypes were shared among *A. rosacea* (7° S) and *A. storchi* (17° S) individuals found approximately 1200 km apart. A single network (figure 3c; fixed 21-step limit connection), covering approximately 25 000 km distance, was recovered for *A. jasoni* ($n = 13$), with 12 haplotypes, of which one was shared between two individuals from SW Pacific basin (16° S, 20° S).

4. Discussion

(a) Delineation of cryptic species in the deep sea

Accounts of cryptic species in the marine realm are no longer new phenomena. Molecular phylogenies often deviate from those relying on traditional taxonomic tools and continue to reveal cryptic diversity [7,21,38,48]. In the deep sea, morphological stasis may not coincide with speciation events owing to stabilizing selection driven by extreme abiotic factors (e.g. low dissolved oxygen, low temperatures and darkness), in turn, introducing challenges in biodiversity estimates [21,49]. In recent years, mtDNA has been a primary tool for the detection of cryptic species [7,50], although the approach remains controversial [51–54], and can be sensitive to sampling [55]. As such, integrative taxonomic approaches (e.g. multi-locus datasets) are recommended [21,56,57]. Morphological taxonomic approaches (e.g. light microscopy, SEM) alone did not allow conclusive identification of new species, as sampling was comprised individuals varying in size and exhibiting variable and/or overlapping morphologies, within and among clades (figure 2 and electronic supplementary material, table S5). Future work based on larger sample sizes and consideration of size-related variation, may reveal species-specific characters. Based on the currently available material, we designate new *Archinome* species on the basis of molecular evidence alone (see also [58]).

Our approach for estimating *Archinome* species diversity was to include broad geographical sampling and to use a multi-locus framework (figure 3). We recognize that our sampling exhibits large geographical gaps (figure 1) leaving an incomplete picture of species distributions. Our phylogenetic

hypothesis for *Archinome* as a whole (figure 3a) required the exclusion of COI third codon position (owing to saturation), resulting in a conflicting topology when the third position was considered (figure 3b). The designation of *A. levinae* n. sp. and *A. tethyana* n. sp. was unambiguous, however, this was less so for the remaining species. In particular, *A. rosacea* appeared to be paraphyletic with respect to *A. storchi* (figure 3a). However, COI was not saturated at more restricted levels, and when the third codon position was included, it became clear that both species were reciprocally monophyletic (figure 3b). Furthermore, these two clades were disparate enough not to form a single haplotype network (figure 3c) and showed a nearly 5% COI divergence. Although we did not find clear morphological differences between *A. rosacea* and *A. storchi* in terms of the argued diagnostic features [40] (figure 2i; for further discussion, see the electronic supplementary material, table S5), we accept both as distinct species. On the same criteria, *A. jasoni* n. sp. was best left as a broadly distributed species (figure 3a–c), despite vast distances separating LOG, CIR and SW Pacific vent populations. COI sequence divergences were less than 4%, with no shared haplotypes. Given this low genetic divergence, the absence of clear morphological distinction and variable age classes among *A. jasoni* n. sp. populations (figure 2d–f), we do not have sufficient evidence to designate them as separate species at this time. We recognize the presence of two, possibly three lineages, as *A. jasoni* n. sp., which only further sampling will be able to resolve.

(b) Distribution and diversification of *Archinome* across chemosynthetic systems

The diversification of *Archinome* appears to align (in part) with Moalic *et al.*'s [5] hypothesis, which proposed west Pacific vent fauna as 'ancestral' and 'central' to those found elsewhere. Our phylogenetic hypothesis deviated with respect to identifying potential links between the Atlantic and eastern Pacific seep/vent communities. However, the biogeographic roles of cold seeps and the Mid-Cayman Spreading Center (MCSC) [59], for example, were not considered in their study. *Archinome jasoni* n. sp. was the sister taxon to the remaining species and included one clade that was exclusive to the SW Pacific basins. Although taxonomic affinities between the CIR and west Pacific have previously been reported [6,42], only a handful of phylogenetic studies have included CIR fauna, and none have evaluated annelids prior to this study. *Archinome jasoni* n. sp. also included a CIR–LOG clade. Van Dover *et al.* [42] proposed CIR as a mid-point for faunal exchange between the Atlantic and west Pacific along the southwest and southeast Indian Ridges, respectively. This scenario appears to be consistent with the presence of *A. jasoni* n. sp. in both regions.

High rates of gene flow and low genetic variation have been reported for *Rimicaris* vent shrimp from 36° N to 4° S [60–64]. Zelnio & Hourdez [64] found west Pacific *Chorocaris vandoverae* as sister to *Rimicaris exoculata* + *Chorocaris chacei* (MAR); however, the phylogenetic placement of CIR *Rimicaris kairei* has not yet been inferred. The gastropod, *Alviniconcha hessleri*, reportedly occurs in the west Pacific and Indian Oceans [42], however *A. aff. hessleri* (CIR) was genetically distinct from its west Pacific counterpart, yet clustered among west Pacific *Alviniconcha* sp. Type 2 [65,66]. A CIR + SW Pacific clade has also been reported for *Bathymodiolus* mussels, showing little

sequence divergences among them [10,11]. Low genetic divergences were also observed among CIR and SW Pacific *A. jasoni* n. sp., and the inclusion of MAR samples now corroborates previously reported affinities among Atlantic, Indian and western Pacific Ocean fauna [5,42]. Unlike widespread *R. exocollata*, we recovered two species in the MAR. However, our limited sampling could have missed the co-occurrence of *A. jasoni* n. sp. and *A. tethyana* n. sp. Alternatively, their colonizing routes leading to A1 and LOG might be significantly separate, and they may never be found in sympatry. Only more extensive sampling will be able to clarify this.

Biogeographic links between the Atlantic and east Pacific were proposed by Van Dover *et al.* [3] and were also observed here in the sister group relationship between the Atlantic *A. tethyana* n. sp. and the eastern Pacific species. Atlantic/east Pacific affinities have been shown for several annelid taxa [1,8,67] pointing towards a former connection between both oceans via a deep ocean passage [68] prior to the closure of the Isthmus of Panama. Recent discoveries of MCSC vent fauna suggest affinities with MAR fauna [59,69], including a new *Rimicaris* species [69] and *Archinome* spp. (A. Glover, 400Q3 personal communication). Although *A. tethyana* n. sp. was sister to the east Pacific clades, its position was not highly supported. This could be attributed to missing data for northern MAR specimens and/or unsampled representatives from intermediate geographical regions (e.g. MCSC; to be evaluated elsewhere).

The diversification of *A. rosacea*, *A. storchi* and *A. levinae* n. sp. is likely attributed to vicariant events involving a formerly widespread ancestor that became isolated from the Atlantic; the latter possibly coincident with the rise of the Central American (CA) Isthmus (approx. 15 Ma; [68]) and subsequent tectonic shifts and subduction events of the Pacific, Cocos and Nazca Plates. The continental margin distribution of *A. levinae* n. sp. may be associated with vicariance coincident with the rise of the CA Isthmus and the formation of the Gulf of California in the Late Miocene (less than 8 Ma; 410Q4 [70,71]). Although records are few, shared GB/CRM species have previously been reported [7,8], and now includes *A. levinae* n. sp. *Archinome* samples from cold seeps at the GB (27°34' N, 111°27' W) were not available for this study, though we suspect *A. levinae* n. sp. may be found there given comparable depths (approx. 1700 m) and being located a mere 50 km north from the GB vent communities [72]. Hydrothermal vents at GB are particular with seeping fluids that circulate through thick sediment layers [73]. The presence of *A. levinae* n. sp. nearly 4000 km south at methane seeps of the CRM suggests either long distance dispersal capacity of larvae or perhaps the presence of overlooked chemosynthetic environments along the CA margin. Genetic isolation between *A. levinae* n. sp. and *A. rosacea/A. storchi*

may have been caused by the formation of the deep Middle American Trench [70] having served as a dispersal barrier to vent populations at GAR (approx. 1000 km south) and the EPR. The genetic break between 7° S and 17° S (SEPR), as seen between *A. rosacea* and *A. storchi*, may be owing to the sampling gap [22] or the result of vicariance associated with the formation and rotation of the Bauer microplate (between 10° and 15° S) in the Miocene [74]. This event has been proposed to have disrupted vent communities and flow of ocean currents along the SEPR, potentially restricting gene flow from more northerly populations (e.g. 7° S; [15]). Compared to other EPR taxa, *Bathymodiolus*, *Lepetodrilus* and *Alvinella*, appear to conform to this trend, whereas species distributions of *Amphisamytha*, *Branchiopolynoe*, *Hesiolyra*, *Riftia* and *Tevnia* appear to be less constrained across this presumed dispersal barrier [8,14,15].

5. Conclusion

We evaluated the phylogeny of *Archinome* from chemosynthetic environments on a global scale to redefine the geographical distribution of *A. rosacea* and *A. storchi*, the former of which had been unclear, and revealed the presence of three previously undescribed cryptic species. Among these, *A. levinae* n. sp., inhabiting both vent and methane seep sites found 4000 km apart and *A. jasoni* n. sp., which for the first time potentially supports biogeographic links among Atlantic, Indian and Pacific Ocean vent systems. With the inclusion of representatives from poorly sampled chemosynthetic sites, in particular CIR and cold seep communities, we hope this study will provide a framework for continued elucidation of the diversification and evolution among deep-sea invertebrate species from chemosynthetic environments.

Acknowledgements. We thank the captains and crews of the R/V *Atlantis*, R/V *Western Flyer*, R/V *Knorr*, R/V *Melville*, R/V *L'Atalante*, R/V *Pourquoi-Pas?* and the pilots of ROVs *Tiburion*, ROVs *Jason I* and *Jason II*, and *Victor 6000* and the pilots and crews of HOVs *Alvin* and *Nautile* for their technical support. Special thanks to Bob Vrijenhoek, chief scientist of the cruises to the SEPR (2005) and SWP (2005), for inviting G.W.R., F.P. and N.G.W. aboard. We are grateful to Didier Jollivet, chief scientist of the *BioSpeedo* 2004 cruise (R/V *L'Atalante*, HOV *Nautile*), Yves Fouquet, chief scientist of the *Serpentine* 2007 cruise (R/V *Pourquoi Pas?* ROV *Victor 6000*) and to Lisa Levin, chief scientist of the CRROCKS cruises (2009; 2010). Thanks also to Bob Vrijenhoek, Rich Lutz, Didier Jollivet and Cindy Van Dover for providing specimens from GB, MAR and CIR. We also thank Dieter Fiege and Gordon Bock for initial discussions on the morphology of *Archinome*. Harim Cha kindly accessioned the material into the SIO-BIC.

Funding statement. Financial support for this study was provided by NSF DBI-0706856, Census of Marine Life TAWNI, SSB Mini-PEET and EOL Rubenstein Fellowship (E.B.), with additional support from DBI-1036186 (A.S.) and OCE-1029160 (G.W.R.).

References

1. Tunnicliffe V, McArthur AG, McHugh D. 1998 A biogeographical perspective of the deep-sea hydrothermal vent fauna. *Adv. Mar. Biol.* **34**, 353–442. (doi:10.1016/S0065-2881(08)60213-8)
2. Desbruyères D, Segonzac M, Bright M. 2006 *Handbook of deep-sea hydrothermal vent fauna*. Linz, Austria: Denisia 18.
3. Van Dover CL, German CR, Speer KG, Parson LM, Vrijenhoek RC. 2002 Evolution and biogeography of deep-sea vent and seep invertebrates. *Science* **295**, 1253–1257. (doi:10.1126/science.1067361)
4. Rogers AD *et al.* 2012 The discovery of new deep-sea hydrothermal vent communities in the southern ocean and implications for biogeography. *PLoS Biol.* **10**, e1001234. (doi:10.1371/journal.pbio.1001234)
5. Moalic Y, Desbruyères D, Duarte CM, Rozenfeld AF, Bachraty C, Arnaud-Haond S. 2011 Biogeography revisited with network theory: retracing the history of hydrothermal vent communities. *Syst. Biol.* **61**, 127–137. (doi:10.1093/sysbio/syr088)

- 442 6. Bachraty C, Legendre P, Desbruyères D. 2008
443 Biogeographic relationships among deep-sea
444 hydrothermal vent faunas at global scale. *Deep-Sea*
445 *Res.* **56**, 1371–1378. (doi:10.1016/j.dsr.2009.
446 01.009)
- 447 7. Johnson SB, Waren A, Vrijenhoek RC. 2008 DNA
448 barcoding of *Lepetodrilus* limpets reveals cryptic
449 species. *J. Shellfish Res.* **27**, 43–51. (doi:10.2983/
450 0730-8000)
- 451 8. Stiller J, Rousset V, Pleijel F, Chevaldonné P,
452 Vrijenhoek RC, Rouse GW. 2013 Phylogeny,
453 biogeography and systematics of hydrothermal vent
454 and methane seep *Amphsamytha* (Ampharetidae,
455 Annelida), with descriptions of three new species.
456 *Syst. Biodivers.* **11**, 35–65. (doi:10.1080/14772000.
457 2013.772925)
- 458 9. Gollner S, Fontaneto D, Martinez Arbujo P. 2011
459 Molecular taxonomy confirms morphological
460 classification of deep-sea hydrothermal vent
461 copepods (Dirivultidae) and suggests broad
462 physiological tolerance of species and frequent
463 dispersal along ridges. *Mar. Biol.* **158**, 221–231.
464 (doi:10.1007/s00227-010-1553-y)
- 465 10. Kyuno A, Shintaku M, Fujita Y, Matsumoto H,
466 Utsumi M, Watanabe H, Fujiwara Y, Miyazaki J.
467 2009 Dispersal and differentiation of deep-sea
468 mussels of the genus *Bathymodiolus* (Mytilidae,
469 Bathymodiolinae). *J. Mar. Biol.* **2009**, 625672.
470 (doi:10.1155/2009/625672)
- 471 11. Miyazaki J, de Oliveira ML, Fujita Y, Matsumoto H,
472 Fujiwara Y. 2010 Evolutionary process of deep-sea
473 *Bathymodiolus* mussels. *PLoS ONE* **5**, e10363.
474 (doi:10.1371/journal.pone.0010363)
- 475 12. Chevaldonné P, Jollivet D, Desbruyères D, Lutz RA,
476 Vrijenhoek RC. 2002 Sister-species of eastern Pacific
477 hydrothermal vent worms (Ampharetidae,
478 Alvinellidae, Vestimentifera) provide new
479 mitochondrial COI clock calibration. *Cah. Biol. Mar.*
480 **43**, 367–370.
- 481 13. Tyler PA, German CR, Ramirez-Llodra E, Van Dover
482 CL. 2002 Understanding the biogeography of
483 chemosynthetic ecosystems. *Oceanol. Acta* **25**,
484 227–241. (doi:10.1016/S0399-1784(02)01202-1)
- 485 14. Hurtado LA, Lutz RA, Vrijenhoek RC. 2004 Distinct
486 patterns of genetic differentiation among annelids
487 of eastern Pacific hydrothermal vents. *Mol. Ecol.*
488 **13**, 2603–2615. (doi:10.1111/j.1365-294X.2004.
489 02287.x)
- 490 15. Plouviez S, Shank TM, Faure B, Daguin-Thiebaut C,
491 Viard F, Lallier FH, Jollivet D. 2009 Comparative
492 phylogeography among hydrothermal vent species
493 along the East Pacific Rise reveals vicariant processes
494 and population expansion in the South. *Mol. Ecol.*
495 **18**, 3903–3917. (doi:10.1111/j.1365-294X.2009.
496 04325.x)
- 497 16. Tyler PA, Young CM. 1999 Reproduction and
498 dispersal at vents and cold seeps. *J. Mar. Biol.*
499 *Assoc. UK* **79**, 193–208. (doi:10.1017/
500 S0025315499000235)
- 501 17. Vrijenhoek RC. 2010 Genetic diversity and
502 connectivity of deep-sea hydrothermal vent
503 metapopulations. *Mol. Ecol.* **19**, 4391–4411.
504 (doi:10.1111/j.1365-294X.2010.04789.x)
18. Shank TM, Lutz RA, Vrijenhoek RC. 1998 Molecular
systematics of shrimp (Decapoda: Bresiliidae) from
deep-sea hydrothermal vents. I: enigmatic 'small
orange' shrimp from the Mid-Atlantic Ridge are
juvenile *Rimicaris exoculata*. *Mol. Mar. Biol.*
Biotechnol. **7**, 88–96.
19. Goffredi SK, Hurtado LA, Hallam S, Vrijenhoek RC.
2003 Evolutionary relationships of deep-sea vent
and cold seep clams (Mollusca: Vesicomidae) of
the 'pacifica/lepta' species complex. *Mar. Biol.* **142**,
311–320. (doi:10.1007/s00227-002-0941-3)
20. Johnson SB, Young CR, Jones WJ, Waren A,
Vrijenhoek RC. 2006 Migration, isolation, and
speciation of hydrothermal vent limpets
(Gastropoda; Lepetodrilidae) across the Blanco
Transform Fault. *Biol. Bull.* **210**, 140–157. (doi:10.
2307/4134603)
21. Vrijenhoek RC. 2009 Cryptic species, phenotypic
plasticity, and complex life history: assessing deep-
sea fauna diversity with molecular markers. *Deep-
Sea Res.* **56**, 1713–1723. (doi:10.1016/j.dsr.2009.
05.016)
22. Audzijonyte A, Vrijenhoek RC. 2010 When gaps
really are gaps: statistical phylogeography of
hydrothermal vent invertebrates. *Evolution* **64**,
2369–2384. (doi:10.1111/j.1558-5646.2010.
00987.x)
23. Cavanaugh CM, Gardiner SL, Jones ML, Jannasch
HW, Waterbury JB. 1981 Prokaryotic cells in the
hydrothermal vent tube worm *Riftia pachyptila*
Jones: possible chemoautotrophic symbionts.
Science **213**, 340–342. (doi:10.1126/science.
213.4505.340)
24. Marsh AG, Mullineaux LS, Young CM, Manahan DT.
2001 Larval dispersal potential of the tubeworm
Riftia pachyptila at deep-sea hydrothermal vents.
Nature **411**, 77–80. (doi:10.1038/35075063)
25. Fisher CR *et al.* 1988 Physiology, morphology, and
biochemical composition of *Riftia pachyptila* at Rose
Garden in 1985. *Deep-Sea Res.* **35**, 1745–1758.
(doi:10.1016/0198-0149(88)90047-7)
26. Fisher CR, Childress JJ, Sanders NK. 1988 The role of
vestimentiferan hemoglobin in providing an
environment suitable for chemoautotrophic sulfide-
oxidizing endosymbionts. *Symbiosis* **5**, 229–246.
27. Grzymalski JJ *et al.* 2008 Metagenome analysis of an
extreme microbial symbiosis reveals eurythermal
adaptation and metabolic flexibility. *Proc. Natl Acad.*
Sci. USA **105**, 17 516–17 521. (doi:10.1073/pnas.
0802782105)
28. Le Bris N. 2007 How does the annelid *Alvinella*
pompejana deal with an extreme hydrothermal
environment? *Rev. Environ. Sci. Biotech.* **6**,
197–221. (doi:10.1007/s11157-006-9112-1)
29. Pradillon F, Gaill F. 2007 Adaptation to deep-sea
hydrothermal vents: some molecular and
developmental aspects. *J. Mar. Sci. Technol.* **15**,
37–53.
30. Gagnière N *et al.* 2010 Insights into metazoan
evolution from *Alvinella pompejana* cDNAs. *BMC*
Genomics **11**, 634. (doi:10.1186/1471-2164-11-634)
31. Jollivet D, Desbruyères D, Bonhomme F, Moraga D.
1995 Genetic differentiation of deep-sea
hydrothermal vent alvinellid populations (Annelida:
Polychaeta) along the East Pacific Rise. *Heredity* **74**,
376–391. (doi:10.1038/hdy.1995.56)
32. Young CR, Fujio S, Vrijenhoek RC. 2008 Directional
dispersal between mid-ocean ridges: deep-ocean
circulation and gene flow in *Ridgeia piscesae*. *Mol.*
Ecol. **17**, 1718–1731. (doi:10.1111/j.1365-294X.
2008.03609.x)
33. Plouviez S, Le Guen D, Lecompte O, Lallier FH,
Jollivet D. 2010 Determining gene flow and the
influence of selection across the equatorial barrier of
the East Pacific Rise in the tube-dwelling polychaete
Alvinella pompejana. *BMC Evol. Biol.* **10**, 220.
(doi:10.1186/1471-2148-10-220)
34. Rousset V, Rouse GW, Feral J-P, Desbruyères D,
Pleijel F. 2003 Molecular and morphological
evidence of Alvinellidae relationships
(Terebelliformia, Polychaeta, Annelida). *Zool. Scr.*
32, 185–197. (doi:10.1046/j.1463-6409.2003.
00110.x)
35. Zottoli RA. 1983 *Amphisamytha galapagensis*, a new
species of ampharetid polychaete from the vicinity
of abyssal hydrothermal vents in the Galapagos Rift,
and the role of this species in rift ecosystems. *Proc.*
Biol. Soc. Wash. **96**, 379–391.
36. Blake JA. 1985 Polychaeta from the vicinity of deep-
sea geothermal vents in the eastern
Pacific. 1. Euprosinidae, Phyllodocidae, Hesionidae,
Nereidae, Glyceridae, Dorvilleidae, Orbinidae, and
Maldanidae. *Bull. Biol. Soc. Wash.* **6**, 67–101.
37. Kudenov JD. 1991 A new family and genus of the
order Amphinomida (Polychaeta) from the
Galapagos hydrothermal vents. In *Proceedings of the*
2nd International Polychaeta Conference (eds
ME Petersen, JB Kirkegaard), *Copenhagen, 1986*.
Systematics, Biology and Morphology of World
Polychaeta. *Ophelia* **5**, 111–120.
38. Barroso R, Klautau M, Sole-Cava AM, Paiva PC. 2010
Eurythoe complanata (Polychaeta: Amphinomidae),
the 'cosmopolitan' fireworm, consists of at least
three cryptic species. *Mar. Biol.* **157**, 69–80.
(doi:10.1007/s00227-009-1296-9)
39. Arhens J, Borda E, Barroso R, Campbell AM, Wolf A,
Nugues M, Paiva P, Rouse GW, Schulze A. 2013 The
curious case of *Hermodice carunculata* (Annelida:
Amphinomidae): genetic homogeneity throughout
the Atlantic Ocean and adjacent basins. *Mol. Ecol.*
22, 2280–2291. (doi:10.1111/mec.12263)
40. Fiege D, Bock G. 2009 A new species of *Archinome*
(Polychaeta: Archinomidae) from hydrothermal
vents on the Pacific Antarctic Ridge 37° S. *J. Mar.*
Biol. Assoc. UK **89**, 689–696. (doi:10.1017/
S0025315409000174)
41. Desbruyères D, Segonzac M. (eds) 1997 *Handbook of*
deep-sea hydrothermal vent fauna. Brest, France:
IFREMER.
42. Van Dover CL *et al.* 2001 Biogeography and ecological
setting of Indian Ocean hydrothermal vents. *Science*
294, 818–823. (doi:10.1126/science.1064574)
43. Levin LA *et al.* 2012 A hydrothermal seep on the
Costa Rica margin: middle ground in a continuum
of reducing ecosystems. *Proc. R. Soc. B* **279**,
2580–2588. (doi:10.1098/rspb.2012.0205)

- 505 44. Fabri MC, Bargain A, Briand P, Gebruk A, Fouquet Y,
506 Morineaux M, Desbruyères D. 2011 Hydrothermal
507 vent community of a new deep-sea field Ashadze-1,
508 12° 58' N on the Mid-Atlantic Ridge and a
509 comparison of all northern Atlantic chemosynthetic
510 ecosystems. *J. Mar. Biol. Assoc. UK* **91**, 1–13.
511 (doi:10.1017/S0025315410000731)
- 512 45. Borda E, Kudenov JD, Beinhold C, Rouse GW. 2012
513 Towards a revised Amphinomidae (Annelida:
514 Amphinomida): description and affinities of a new
515 genus and species from the Nile deep-sea Fan,
516 Mediterranean Sea. *Zool. Scr.* **41**, 307–325. (doi:10.
517 1111/j.1463-6409.2012.00529.x)
- 518 46. Nygren A, Pleijel F. 2011 From one to ten in a
519 single stroke: resolving the European *Eumida*
520 *sanguinea* (Phyllodoceidae, Annelida) species
521 complex. *Mol. Phylogenet. Evol.* **58**, 132–141.
522 (doi:10.1016/j.ympev.2010.10.010)
- 523 47. Clement M, Posada D, Crandall KA. 2000 TCS: a
524 computer program to estimate gene genealogies.
525 *Mol. Ecol.* **4**, 331–346.
- 526 48. Knowlton N. 2000 Molecular genetic analyses of
527 species boundaries in the sea. *Hydrobiologia* **420**,
528 73–90. (doi:10.1023/A:1003933603879)
- 529 49. Bickford D, Lohman DJ, Sodhi NS, Ng PKL, Meier R,
530 Winker K, Ingram KK, Das I. 2007 Cryptic species as
531 a window on diversity and conservation. *Trends Ecol.*
532 *Evol.* **22**, 148–155. (doi:10.1016/j.tree.2006.11.004)
- 533 50. Hebert PD, Penton EH, Burns JM, Janzen DH,
534 Hallwachs W. 2004 Ten species in one: DNA
535 barcoding reveals cryptic species in the neotropical
536 skipper butterfly *Astrartes fulgerator*. *Proc. Natl*
537 *Acad. Sci. USA* **101**, 14 812–14 817. (doi:10.1073/
538 pnas.0406166101)
- 539 51. Meyer CP, Paulay G. 2005 DNA barcoding: error rates
540 based on comprehensive sampling. *PLoS Biol.* **3**,
541 e422. (doi:10.1371/journal.pbio.0030422)
- 542 52. Cameron S, Rubinoff D, Will K. 2006 Who will
543 actually use DNA barcoding and what will it cost?
544 *Syst. Biol.* **55**, 844–847. (doi:10.1080/10635150
545 600960079)
- 546 53. Rubinoff D, Cameron S, Will K. 2006 A genomic
547 perspective on the shortcomings of mitochondrial
548 DNA for 'barcoding' identification. *J. Hered.* **97**,
549 581–594. (doi:10.1093/jhered/esl036)
- 550 54. Moritz C, Cicero C. 2004 DNA barcoding: promise
551 and pitfalls. *PLoS Biol.* **2**, e354. (doi:10.1371/
552 journal.pbio.0020354)
- 553
554
555
556
557
558
559
560
561
562
563
564
565
566
567
55. Wiemers M, Fiedler K. 2007 Does the DNA
barcoding gap exist? A case study in blue butterflies
(Lepidoptera: Lycaenidae). *Front. Zool.* **4**, 8. (doi:10.
1186/1742-9994-4-8)
56. Will KW, Mishler BD, Wheeler QD. 2005 The perils
of DNA barcoding and the need for integrative
taxonomy. *Syst. Biol.* **54**, 844–851. (doi:10.1080/
10635150500354878)
57. Dasmahapatra KK, Elias M, Hill RI, Hoffman JI,
Mallet J. 2010 Mitochondrial DNA barcoding detects
some species that are real, and some that are not.
Mol. Ecol. Resour. **10**, 264–273. (doi:10.1111/j.
1755-0998.2009.02763.x)
58. Cook LG, Edwards RD, Crisp MD, Hardy NB. 2010
Need morphology always be required for new
species descriptions? *Invert. Syst.* **24**, 322–326.
(doi:10.1071/IS10011)
59. Connelly DP *et al.* 2012 Hydrothermal vent fields
and chemosynthetic biota on the world's deepest
seafloor spreading centre. *Nat. Commun.* **3**, 620.
(doi:10.1038/ncomms1636)
60. Williams AB, Rona PA. 1986 Two new caridean
shrimps (Bresiliidae) from a hydrothermal field on
the Mid-Atlantic Ridge. *J. Crus. Biol.* **6**, 446–462.
(doi:10.2307/1548184)
61. Shank TM, Black MB, Halanych KM, Lutz RA,
Vrijenhoek RC. 1999 Miocene radiation of deep-sea
hydrothermal vent shrimp (Caridea: Bresiliidae):
evidence from mitochondrial cytochrome oxidase
subunit I. *Mol. Phylogenet. Evol.* **13**, 244–254.
(doi:10.1006/mpev.1999.0642)
62. Teixeira S, Serrão EA, Arnaud-Haond S. 2012
Panmixia in a fragmented and unstable
environment: the hydrothermal shrimp *Rimicaris*
exoculata disperses extensively along the Mid-
Atlantic Ridge. *PLoS ONE* **7**, e38521. (doi:10.1371/
journal.pone.0038521)
63. Teixeira S. 2010 Recent population expansion and
connectivity in the hydrothermal shrimp *Rimicaris*
exoculata along the Mid-Atlantic Ridge. *J. Biogeogr.*
38, 564–574. (doi:10.1111/j.1365-2699.2010.
02408.x)
64. Zelnio KA, Hourdez S. 2009 A new species of
Alvinocarid (Crustacea: Decapoda: Caridea:
Alvinocarididae) from hydrothermal vents at the
Lau Basin, southwest Pacific, and a key to the
species of Alvinocarididae. *Proc. Biol. Soc. Wash.*
122, 52–71. (doi:10.2988/07-28.1)
65. Kojima S, Fujikura K, Okutani T, Hashimoto J. 2004
Phylogenetic relationship of *Alviniconcha* gastropods
from the Indian Ocean to those from the Pacific
Ocean (Mollusca: Provannidae) revealed by
nucleotide sequences of mitochondrial DNA. *Venus*
63, 65–68.
66. Suzuki Y *et al.* 2006 Host–symbiont relationships in
hydrothermal vent gastropods of the genus
Alviniconcha from the southwest Pacific. *Appl.*
Environ. Microb. **72**, 1388–1393. (doi:10.1128/AEM.
72.2.1388-1393.2006)
67. Black MB, Halanych KM, Maas PAY, Hoeh WR,
Hashimoto J, Desbruyères D, Lutz RA, Vrijenhoek RC.
1997 Molecular systematics of vestimentiferan
tubeworms from hydrothermal vents and cold-water
seeps. *Mar. Biol.* **130**, 141–149. (doi:10.1007/
s002270050233)
68. Burton KW, Ling H-F, O'Nions RK. 1997 Closure of
the Central American Isthmus and its effect on
deep-water formation in the North Atlantic. *Nature*
386, 382–385. (doi:10.1038/386382a0)
69. Nye V, Copley J, Plouviez S. 2011 A new species of
Rimicaris (Crustacea: Decapoda: Caridea:
Alvinocarididae) from hydrothermal vent fields on
the Mid-Cayman Spreading Centre, Caribbean.
J. Mar. Biol. Assoc. UK **92**, 1057–1072. (doi:10.
1017/S0025315411002001)
70. Helenes J, Carreno AL, Carrillo RM. 2009 Middle to
Late Miocene chronostratigraphy and development
of the northern Gulf of California. *Mar.*
Micropaleontol. **72**, 10–25. (doi:10.1016/j.
marmicro.2009.02.003)
71. Fisher RL. 1961 Middle America trench; topography and
structure. *Geol. Soc. Am. Bull.* **72**, 703–719. (doi:10.
1130/0016-7606(1961)72[703:MATTAS]2.0.CO;2)
72. Simoneit BRT, Lonsdale PF, Edmond JM, Shanks III
WC. 1990 Deep-water hydrocarbon seeps in
Guaymas Basin, Gulf of California. *Appl. Geochem.* **5**,
41–49. (doi:10.1016/0883-2927(90)90034-3)
73. Lonsdale P, Becker K. 1985 Hydrothermal plumes,
hot springs, and conductive heat flow in the
Southern Trough of Guaymas basin. *Earth Planet.*
Sci. Lett. **73**, 211–225. (doi:10.1016/0012-
821X(85)90070-6)
74. Eakins BW, Lonsdale PF. 2003 Structural patterns
and tectonic history of the Bauer microplate, eastern
tropical Pacific. *Mar. Geophys. Res.* **24**, 171–205.
(doi:10.1007/s11001-004-5882-4)

Electronic Supplementary Material:

Cryptic species of *Archinome* (Annelida: Amphinomida) from vents and seeps

Elizabeth Borda^{1,10*}, Jerry D. Kudenov², Pierre Chevaldonné³, James A. Blake⁴, Daniel Desbruyères⁵, Marie-Claire Fabri⁵, Stéphane Hourdez⁶, Fredrik Pleijel⁷, Timothy M. Shank⁸,
Nerida G. Wilson⁹, Anja Schulze¹⁰ and Greg W. Rouse^{1*}

¹*Scripps Institution of Oceanography, La Jolla, California, 92034, USA*

²*University of Alaska Anchorage, Anchorage, Alaska, 99508 USA*

³*CNRS - UMR 7263 IMBE, Institut Méditerranéen de la Biodiversité et d'Ecologie Marine et Continentale, Aix-Marseille Université, Station Marine d'Endoume, Rue de la Batterie des Lions, 13007 Marseille, France*

⁴*Marine and Coastal Research Center, AECOM, Woods Hole, Massachusetts, 02543 USA.*

⁵*Département Etude des Ecosystèmes Profonds, Centre de Brest de l'IFREMER, 29280 Plouzané Cedex, France*

⁶*CNRS-UPMC UMR 7127, Station Biologique de Roscoff, 29682 Roscoff, France*

⁷*University of Gothenburg, Tjörnö, Strömstad, Sweden*

⁸*Woods Hole Oceanographic Institution, Woods Hole, Massachusetts 02543 USA*

⁹*The Australian Museum, Sydney, NSW 2010, Australia*

¹⁰*Texas A&M University at Galveston, Galveston, TX, 77553, USA*

*Corresponding authors: lizborda@gmail.com; grouse@ucsd.edu

PDF includes:

Materials and Methods: Additional gene data collection and phylogenetic methods

Materials and Methods: Morphological Evaluation

Results: Systematics

Discussion

References

Table S1

Table S2

Table S3

Table S4

Table S5

Figure Legends

Figure S1

Figure S2

Figure S3

Figure S4

MATERIALS AND METHODS

Additional gene data collection and phylogenetic methods

Use of COI Folmer primers [1] occasionally resulted in the co-amplification of non-symbiotic, γ -proteobacteria [2, 3], therefore, alternative degenerate primers [4] and/or *Archinome* specific primers were used (Table S2). Sequences were analyzed using an ABI PRISM[®] 3730 (Applied Biosystems, Inc.) at the University of Hawaii at Manoa Advanced Studies in Genomics, Proteomics and Bioinformatics and an ABI PRISM[®] 3130 at the Texas A&M University at Galveston Marine Genomics Lab. All gene fragments were aligned using MUSCLE [5, 6] and visualized and trimmed using MESQUITE 2.71 [7]; COI was also visualized and aligned according to amino acid translation. jModelTest [8] was used to infer appropriate evolutionary models for each gene [88 models: COI: TrN+I; 16S: GTR+I+G; 28S: TIM1+G; ITS1: TIM2+I; 24 models: COI/16S: GTR+I+G; 28S: GTR+G; ITS1: HKY+I] as selected by the Akaike information criterion. DAMBE [9] was used to estimate COI saturation via saturation plots of transitions/transversions against TrN corrected genetic distances. MEGA 5 [10] was used to calculate TrN corrected and uncorrected pairwise distances.

Morphological Evaluation

Specimens evaluated for morphology ranged between 0.2 mm–38 mm in length, with a minimum of 5 and maximum of 36 chaetigers; truly large individuals (>20 mm) were exceedingly rare by comparison to the vast preponderance that were <10 mm in length. The greatest morphological variation was present in the position of the anus on terminal chaetigers. All *Archinome* specimens are consistent with the re-description proposed by Kudenov [11], however certain taxonomic terminology needs clarification. The usage of “dorsal” cirri *sensu*

Kudenov [11] and “lateral” cirri *sensu* Kudenov [11] and Fiege and Bock [12], describing the dorsal most cirri in *Archinome* (and other amphinomids) has led to confusion in assessing homology with respect to other annelid groups, which typically only have dorsal and ventral cirri [13]. The ciliated “dorsal” cirri of *Archinome* lack a blood vessel and are always associated with dorsal branchiae. Thus, the “dorsal” cirrus [11; 12], should be referenced as the “accessory dorsal” cirri *sensu* Yáñez-Rivera and Carrera-Parra [14], while vascularized “lateral” cirri [11, 12] are homologous to the “true” dorsal cirri of other annelids [13]. Images of live and preserved specimens were taken with a Nikon E4300, Canon PowerShot G9 or Canon EOS REBEL T1i cameras on Leica MZ8 or MZ9.5 stereomicroscopes. Images were edited and figures were made using Adobe® Illustrator® CS3 and Adobe® Photoshop® CS3 (Adobe® Systems, Inc). Specimens evaluated for morphology are deposited in the US National Museum of Natural History (USNM), Senckenberg Museum Frankfurt (SMF) and Scripps Institution of Oceanography Benthic Invertebrate Collection (SIO-BIC).

RESULTS

Morphological Results

Archinome specimens studied were consistent with the general diagnoses of *A. rosacea* (and *A. storchi*; Fig. S1). We compared key diagnostic features [11, 12], which were expanded to include other traits (Table S4-S5) among *Archinome* specimens from different geographic regions and clades. While anatomical differences exist, based on the material presently available we found little consistent evidence to delineate species on the basis of morphology alone. Despite large geographic and/or ecological distances separating the *Archinome* specimens sampled, morphological variation appeared to be inconsistent and generally associated with

segmental stage and size. Of the 54 morphological traits included here (Table S5), 28 were common to all specimens examined. The remaining 26 traits exhibited variation of which 8 branchial and chaetal features (Table S4: 36-37, 40-42, 46-48) tend to be less subject to preservation artifacts, a selection of which are addressed below. Thus, the normally reliable morphological characters used in the systematics of Amphinomida [15, 16] largely overlap and provide little consistent support in the delineation of *Archinome* species (Table S5).

Median antenna

The form and length of the median antenna have been emphasized as key diagnostic characters to distinguish *A. storchi* and *A. rosacea*. It was found to be cirriform in *A. rosacea* (GAR1, USNM 81788), *A. storchi* (SEPR, SIO-BIC A3543; PAR, SMF 17876) and *A. levinae* n. sp. (CRM, SIO-BIC A1316), but conical in small *A. rosacea* (GAR2, USNM 1221442). However, the median antenna is similarly short in both *A. rosacea* and *A. levinae* n. sp., and long in *A. storchi*. Likewise, the median antenna of *A. jasoni* n. sp. (CIR, SIO-BIC A3544; SWP, SIO-BIC A3546-47) was cirriform (sometimes claviform), but papilliform in large specimens of *A. jasoni* n. sp. (MAR, SIO-BIC A3548); all are generally short to minute. These data led us to surmise that median antenna form and length likely have limited value as a systematic feature in this genus.

Dorsal anus

The position of the dorsal anus, which was described as the main diagnostic feature separating *A. rosacea* from *A. storchi* (originally noted as chaetiger 17 vs. 19, respectively), was not consistent within and among clades relative to the results recovered by molecular data. The dorsal position of the anus appeared to be size/segmental stage dependent and unreliable for clear species diagnoses. In the case of *A. storchi*, which was originally described from a 23-chaetiger

specimen, the dorsal anus position was not consistent among our sampling of SEPR representatives, where the majority were <23 chaetigers specimens and with an anus position location similar to *A. rosacea* (e.g., Fig. 3I). However, the dorsal anus of *A. rosacea* specimens with up to 23 chaetigers (including “reduced” posterior segments) from North East Pacific Rise was positioned on chaetiger 18 and extended through 2 to 3 chaetigers, clearly overlapping that of *A. storchi* (Table S5). Examining this character across specimens of other *Archinome* species also was found to be variable in larger specimens (>23 chaetigers). For instance, the dorsal anus of *A. jasoni* n. sp. commenced on chaetiger 21 or 22, and continued through 3 or 4 chaetigers in MAR (14°N) and CIR specimens, respectively (Table S5). In MAR (23°N) specimens of *A. tethyana* n. sp. (SIO-BIC A3548), the dorsal anus, first situated on chaetiger 25, coursed through 3 chaetigers, whereas that of *A. levinae* n. sp. overlapped the placement of those in both *A. rosacea* and *A. storchi* (Table S5).

Branchia

The number of branchial filaments present on the first gill was used to distinguish *A. rosacea* and *A. storchi* [12]. However, this character appeared to be dependent on size/segmental stage, and likely not highly informative. For example, filaments numbered 1 or 3 per first gill in small (GAR1, 2; SEPR) and large specimens (NEPR; PAR) of *A. rosacea* and *A. storchi*, respectively; they also numbered 3 in large *A. levinae* n. sp. (CRM). By comparison, the branchial filaments of *A. jasoni* n. sp. (CIR; SWP; MAR) totaled 2-5 compared to 4 in *A. tethyana* n. sp. (MAR). Thus, the separation of *A. storchi* and *A. rosacea* was not supported based on the number of filaments in the first branchia. Moreover, the broad overlap between the various specimens examined strongly suggested that this trait is likely size/segmental stage dependent.

Maximal numbers of branchial filaments in mid-body segments were also used to distinguish *A. storchi* from *A. rosacea* [12]. However, this trait also appeared to partly be size- and perhaps habitat-dependent [see also 17]. While a maximum of 8 and 7 filaments per branchia were detected in comparably sized specimens of *A. rosacea* and *A. storchi*, respectively, more than 15 filaments per gill were present in *A. levinae* n. sp. Those of *A. jasoni* n. sp. (CIR) also numbered 15-16 filaments per gill, in direct contrast to 4-5 in MAR and SWP specimens of *A. jasoni* n. sp.; 7-9 filaments were maximally present per mid-body chaetiger of *A. tethyana* n. sp.

Midventral scutes

Anterior midventral scutes exhibited varying degrees of fusion such that annular rings between them were either partially or completely absent. Scutes of chaetigers 2-3 were typically distinct and separate in small specimens of all examined *Archinome* specimens generally, and typified by both *A. rosacea* (GAR) and *A. storchi* (SEPR). Those of chaetigers 2-3 are generally fused in larger specimens of *A. rosacea*, *A. storchi* and *A. levinae* n. sp., although chaetiger 4 was also partly fused in *A. rosacea* (SIO-BIC A3543). Similarly, scutes of chaetigers 2-4 were fused in specimens of *A. jasoni* n. sp. (CIR, SWP) from the Indo-Pacific, compared to chaetigers 2-5 in Atlantic specimens of *A. jasoni* n. sp. (MAR) and *A. tethyana* n. sp. In our opinion, fusion of contiguous anterior scutes appeared to be an size/segmental stage dependent character in the delineation of *Archinome* species.

Caruncle

Caruncle form and placement are central to the systematics of Amphinomida [15, 16], but seemed to be of limited usefulness in differentiating *Archinome* species. In the former case, all were elongate and trilobed (Fig. S1). In the latter instance, caruncles in large specimens extended to chaetiger 3 in *A. levinae* n. sp. in contrast to chaetigers 4-5 in *A. rosacea* and *A. storchi*.

Caruncle placement in large *A. levinae* n. sp. is similar to that in small specimens of both *A. rosacea* (GAR) and *A. storchi*. Comparably, caruncles generally reached chaetiger 3 (or to 5) in *A. jasoni* n. sp. (CIR, MAR, SWP) or chaetigers 3-4 in *A. tethyana* n. sp. (MAR).

Chaetae

Measurements of long and short “prongs” of bifurcate chaetae [18] have proved useful in the systematics of Amphinomida [19]. However, measurements of prong ratios were generally similar among specimens of comparable size, variable among size classes, and appeared to be of limited applicability as morphological species characters.

Prong angles have only recently been used in amphinomid systematics [19] and newly applied here with mixed results (Table S5). Measurements of notochaetal angles were 23° in *A. rosacea*, *A. storchi* and *A. levinae* n. sp., while neurochaetal angles were 22° in the former two taxa, and unavailable in the latter; values do not support morphological differences between these taxa. However, juvenile *A. rosacea* (GAR) consistently displayed highly divergent prong angles. Similarly, noto- and neurochaetal prong angles were 31° and 24°, respectively, in *A. jasoni* n. sp. (CIR, SWP, MAR), although neurochaetae of SWP specimens had larger angles. This character may provide useful information in future, but not in the present context.

Calculations of triangular areas formed by prongs of bifurcate chaetae (chaetal areas) were developed as new meristic characters to differentiate *Archinome* species (Table S4). That is, notochaetal areas estimated for large *A. rosacea*, *A. levinae* n. sp., and *A. storchi* were 8, 7.1, and $1.8 \times 10^3 \mu\text{m}^2$, respectively. Neurochaetal values of *A. rosacea* and *A. storchi* ranged up to 5.2 and $1.6 \times 10^3 \mu\text{m}^2$; data for *A. levinae* n. sp. were unavailable. These area estimates produced results suggesting that *A. rosacea* is similar to *A. levinae* n. sp., both of which differed from *A. storchi*. However, chaetal areas in small specimens of *A. rosacea* and *A. storchi* differed

consistently. By comparison, estimates of notochaetal areas for *A. jasoni* n. sp. (CIR, SWP) were generally lower, notwithstanding high values in SWP specimens; whereas those for *A. jasoni* n. sp. (MAR) were notably smaller. Neurochaetal areas of *A. jasoni* n. sp. ranged from 3-5.4 x10³ μm² (CIR, SWP) and 3.5 x10³ μm² (MAR). Noto- and neurochaetal area estimates of *A. tethyana* n. sp. (MAR) were 2.6 and 2.4 x10³ μm². These characters generally did not provide consistently meaningful insights leading to a resolution of *Archinome* species, and reinforced our surmise that morphological variability in this feature is largely associated with size/segmental stage.

Pygidial “eyespot”

The presence of pygidial pigmentation, also referred to as “eyespot” [11] was one of the more reliable morphological traits that may vary geographically. However, pigmentation patterns appeared to fade over time in alcohol-stored specimens. The “eyespot” in *A. rosacea*, *A. storchi* and *A. levinae* n. sp. were present as a single lateral stripe of pigment [11] that did not continue around the tip of the pygidial cirrus; pigmented areas were not detectable in preserved juvenile *A. rosacea* and *A. storchi*. This morphological character did not differentiate between the three taxa, in contrast to that provided by the molecular data. Pygidial “eyespot” in *A. jasoni* n. sp. (CIR, MAR) were present as a terminal distal patch of pigment restricted to the distal tip of the cirrus; pigment patterns appeared larger and more diffuse in MAR specimens, and were not detectable in SWP specimens. The “pygidial eyespot” of *A. tethyana* n. sp. were present as a dorsal patch of pigment extending from base to distal tip of the cirrus. The latter two species seemed to lack the highly defined pigmentation patterns present in *A. rosacea*, *A. storchi* and *A. levinae* n. sp.; it is surmised that alcohol leaches pygidial pigments.

Systematics

Genus *Archinome* Kudenov, 1991

Type species: Euphrosine rosacea Blake 1985

Species included: Archinome rosacea (Blake, 1985), *Archinome storchi* Fiege and Bock, 2009, *Archinome jasoni* n. sp., *Archinome tethyana* n. sp. and *Archinome levinae* n. sp.

Diagnosis: Body short, fusiform, with mid-ventral scutes, up to 38 segments; iridescent purple or pink (live; Fig 2). Prostomium, bearing five appendages including median antenna arising from anterior part of caruncle, antennae and palps. Dark, deeply embedded pigmentation “eyespot,” numbering two pairs. Caruncle, narrow, elongate and trilobed, fused to body at chaetiger 2 (chaetal segments), unattached thereafter. Segmental lobes large and laterally bursiform. Parapodia biramous, notopodia and neuropodia well separated. Notochaetal fascicles arrayed in radial whorls. Dorsal, accessory dorsal and ventral cirri present on all segments, except terminal chaetigers. Ramified branchiae, digitiform tuft, first appearance on chaetiger 3 (Fig. 2B, C, E, I). Chaetae bifurcate. Anus position dorsal on posterior chaetigers. Pygidium with unpaired median cirrus.

Distribution: Pacific, Atlantic and Indian Oceans. Recorded from the East Pacific Rise (including Pacific Antarctic Ridge), Guaymas Basin, Galapagos Rift, Mid Atlantic Ridge, Mid Cayman Spreading Center, Central Indian Ridge, southwest Pacific basins and the Costa Rica Margin.

Habitat: Hydrothermal vents and cold methane seeps.

Biology: Inhabits the crevices and surfaces of deep-sea mussel beds, tubeworm and/or near shrimp aggregations. Active predator and carnivore of mollusks, crustaceans and other polychaetes [20]. The eversible ventral proboscis, armed with transverse ridges, is used to capture prey. When disturbed, will assume a defensive posture by curling its body dorsoventrally

displaying expansive chaetae, looking like a hedgehog or porcupine.

Remarks: The generic diagnosis of *Archinome* is emended here to correct an error in the original description [11], where branchiae in *A. rosacea* begin from chaetiger 3, and not from chaetiger 2 as originally stated and tend to lack them on the last 1-2 segments.

Archinome rosacea (Blake, 1985)

Euphrosine rosacea Blake, 1985

Archinome rosacea Kudenov, 1991

Type Locality: Rose Garden, Galapagos Rift

Material examined: USNM 81788 (HOLOTYPE); USNM 81789 (PARATYPES; n=150); USNM 81790-92; USNM 1221442.

Molecular vouchers: WHOI 4115-3-[1-6], Rose Bud, Galapagos Rift, 00°46'16"N, 86°13'36"W, 2451 m, low temperature vents, *Alvin* Dive 4115 (AT-11), COLL: Tim Shank; SIO-BIC A2875-A2877, North East Pacific Rise, 09°46'25"N, 104°16'40"W, 2505 m; high temperature vents; *Alvin* Dive 3763, COLL: Tim Shank; SIO-BIC A2881-A2882, North East Pacific Rise, *Nautila* Dive 1738, COLL: Stéphane Hourdez; SIO-BIC A2883, North East Pacific Rise, *Nautila* Dive 1742, COLL: Stéphane Hourdez; SIO-BIC A2890, Yaquina, South East Pacific Rise, 07°25'14"S, 107°47'41"W, 2746 m; *Nautila* Dive 1572, COLL: Stéphane Hourdez; SIO-BIC A2891, Yaquina, South East Pacific Rise, 07°22'14"S, 107°47'07"W, 2719 m; *Nautila* Dive 1571, COLL: Stéphane Hourdez; SIO-BIC A2862, Sarah Spring, South East Pacific Rise, 07°25'S, 107°47'W, 2750 m; *Nautila* Dive 1573, COLL: Stéphane Hourdez.

Diagnosis: Morphology – as described for genus. Genetics – Sequences from WHOI4115-3-3 are designated as diagnostic for *A. rosacea*: COI (JX028059), 16S (JX027994), 28S (JX028122)

and ITS1 (KF288955). Intraspecific range: $d_{COI} = 0.0\text{--}0.9\%$. Interspecific range: $d_{COI} = 4.3\text{--}18.3\%$.

Distribution [Emended]: East Pacific Ocean. Galapagos Rift, East Pacific Rise from at least 9°N to 7°S. Depth range: ~2400 – 2750 m.

Habitat: Hydrothermal vents.

Remarks: *Archinome rosacea* is distinguished from other *Archinome* species geographically (Fig. 1), as a clade (IV) (Fig. 2) and by being at least 4% divergent from other species.

Archinome rosacea was originally collected from Rose Garden. However, when scientists returned to this site in 2002 they discovered that Rose Garden had been destroyed by volcanic activity [21]. Therefore, genetic data from the original type locality do not exist, therefore we provide genetic data from Rosebud, located ~300 km northwest from the former Rose Garden. Live images of *A. rosacea sensu stricto* are not available and only formalin preserved material was available from the type locality. Based on the current representatives, at this time we find a restricted range for *A. rosacea* to Galapagos Rift, the northern South East Pacific Rise and North East Pacific Rise to at least 9°N.

Archinome storchi Fiege and Bock, 2009

(Fig. 3I)

Type Locality: Pacific Antarctic Ridge

Material examined: HOLOTYPE – SMF17876; SIO-BIC A3543

Molecular vouchers: SIO-BIC A2389, Oasis Vent, SEPR, 17°25'23"S, 113°12'17"W, 2585 m; *Nautila* Dive 1590, COLL: Stéphane Hourdez; SIO-BIC A2353-2354, SEPR, 23°32'46"S, 115°34'10"W, 2598 m; *Alvin* Dive 4096 (AT-11), COLL: Greg Rouse, Nerida Wilson; SIO-BIC

A2355-A2357, SEPR, 31°51'47"S, 112°02'32"W, 2334 m; *Alvin* Dive 4092 (AT-11), COLL: Greg Rouse, Nerida Wilson; SIO-BIC A2359-A2361, SEPR, 31°00'54"S, 111°55'55"W, 2334 m; *Alvin* Dive 4094 (AT-11), COLL: Greg Rouse, Nerida Wilson; SIO-BIC A2316-A2317, German Flats, SEPR, 37°47'33"S, 110°54'57"W, 2216 m; high temperature vents; *Alvin* Dive 4088, COLL: Greg Rouse, Nerida Wilson; SIO-BIC A2318, German Flats, SEPR, 37°47'29"S, 110°54'51"W, 2220 m; *Alvin* Dive 4090, COLL: Greg Rouse, Nerida Wilson.

Diagnosis: Morphology – as described for genus. Genetics – Sequences from SIO-BIC A2318 are designated as diagnostic for *A. storchi*: COI (JX028067), 16S (JX028002), 28S (JX028125) and ITS1 (KF288937). Intraspecific range: $d_{\text{COI}} = 0.0\text{--}1.1\%$. Interspecific range: $d_{\text{COI}} = 4.3\text{--}17.4\%$.

Distribution [Emended]: Southeast Pacific Ocean. South East Pacific Rise, from at least 17°S–31°S (Fig. 1) and Pacific Antarctic Ridge. Depth range: 2200–2900 m.

Habitat: Hydrothermal vents.

Remarks: With respect to morphology, the diagnostic feature established for *A. storchi* (position of the anus in the holotype, a 23 chaetiger specimen, was not found to reliably distinguish *A. storchi* and *A. rosacea*, particularly in juvenile specimens (<22 chaetigers). This feature was found to be size dependent (i.e., number of chaetigers) and to overlap with *A. rosacea*. Genetically, we distinguished *A. storchi* from *A. rosacea* on the basis of reciprocal monophyly between from Pacific Antarctic Ridge and Galapagos Rift representatives (COI and COI_{ALL}+16S+28S+ITS1) and with d_{COI} ranging 4.3-5.7% (Fig. 3; Table 1). We recognize that an average sequence divergence of 5%, the presence of overlapping diagnostic characters with *A. rosacea*, and the lack of reciprocal monophyly with *A. rosacea* in 16S, 28S and ITS1, would otherwise not support the designation of separate species, however, given that *A. storchi* has

been previously designated and there is no evidence for taxonomic overlap in the South East Pacific Rise, we choose to retain the name *A. storchi* for Clade V. We expand the distributional range of *A. storchi* to at least 17°S along the South East Pacific Rise (Fig. 1), therefore, the sequenced specimen from 17°S in Wiklund et al. [23] is identified as *A. storchi*, instead of *A. rosacea*.

***Archinome jasoni*, new species**

Type Material: HOLOTYPE – SIO-BIC A2375, Tui Malila Lau, South West Pacific Lau Basin, 21°59'N, 176°34'E, 1900 m, 16 May 2005, 1 specimen preserved in 95% Ethanol, *Jason 2* Dive 140, COLL: Greg Rouse. PARATYPES – SIO-BIC A2376-A2377, Tui Malila Lau, South West Pacific Lau Basin, 21°59'N, 176°34'E, 1900 m, 16 May 2005, 2 specimen preserved in 95% Ethanol, *Jason 2* Dive 140, COLL: Greg Rouse; SIO-BIC A2365-2367, White Lady, North Fiji, South West Pacific Lau Basin, 16°59'N, 173°54'E, 1985 m, 27 May 2005, 3 specimens preserved in 95% Ethanol, *Jason 2* Dive 149, COLL: Greg Rouse; SIO-BIC A2369-2371, Kilo Moana Lau, South West Pacific Lau Basin, 20°59'N, 173°54'E, 2650. SIO-BIC A2313-A2315, Kairei Field, Central Indian Ridge, 25°19'N, 70°02'E, 2432 m, 7 April, 2001, 3 specimens preserved in 80% Ethanol, *Jason 1S* Dive 297, COLL: Greg Rouse.

Diagnosis: Morphology – As described for genus. Genetic data – Sequences from SIO-BIC A2375 (COI: JX028092; 16S: JX028027; 28S: JX028131; ITS: KF288946) and SIO-BIC A2313 (COI: JX028064; 16S: JX027999; 28S: JX028124; ITS: KF288935) are designated as the genetic diagnoses for each of the two *A. jasoni* n. sp. clades, respectively. Intraspecific range: $d_{\text{COI}} = 0.0\text{--}3.6\%$. Interspecific range: $d_{\text{COI}} = 10.4\text{--}18.3\%$.

Type Localities: Tui Malila Lau, South West Pacific Lau Basin.

Distribution: Atlantic, Indian and southwest Pacific Oceans. Depth range: ~1900–3040 m.

Habitat: Hydrothermal vents.

Etymology: Named after ROVs *Jason I* and *Jason II/Medea*, which were used to collect specimens studied here.

Remarks: *Archinome jasoni* n. sp. is distinguished from other *Archinome* species geographically (Fig. 1), as a clade I (Fig. 3) and by being at least 10% divergent (COI) from other *Archinome* species. In addition, the evaluation of COI+16S supported a single network (starting at a fixed 21-step connection limit; compared to a fixed connection limits greater than 50 for the *rosacea/storchi* split) for populations representing the southwest Pacific basins, the Indian and Atlantic oceans. Therefore, we took a conservative approach and accept a broad distribution for *A. jasoni* n. sp., until additional sampling becomes available. Voucher material for *A. jasoni* n. sp. from Logatchev is unavailable.

***Archinome tethyana*, new species**

Type Material: HOLOTYPE – SIO-BIC A2871, Ashadze-1, Mid Atlantic Ridge, 12°58'N, 44°51'W, 4080 m, 2010, 1 specimen preserved in 95% Ethanol, *Victor6000* Dive 312, COLL: Marie-Claire Fabri. PARATYPES – SIO-BIC A2872-A2874, Ashadze-1, Mid Atlantic Ridge, 12°58'N, 44°51'W, 4080 m, 2010, 3 specimens preserved in 95% Ethanol, *Victor6000* Dive 312, COLL: Marie-Claire Fabri.

Type Locality: Ashadze-1, 12° N, MAR (4080 m).

Diagnosis: *Morphology* – as described for genus. *Genetics* – Sequences from SYNTYPES SIO-BIC A2874 (COI: JX028114; 16S: JX028055; 28S: JX028140) and SIO-BIC A2871 (16S: JX028052; ITS: KF288958) are designated as the genetic diagnoses for *A. tethyana*. Interspecific range: $d_{\text{COI}} = 10.4\text{--}15.3\%$.

Distribution: Northern Atlantic Ocean. Mid Atlantic Ridge. Depth range: 3000–4080 m.

Habitat: Hydrothermal vents.

Etymology: The specific epithet is derived from the Tethys Seaway, which formally connected the Pacific and Atlantic basins and circulated around the equator. The Tethys is symbolic for the “intermediate” phylogenetic position *A. tethyana* n. sp. between eastern and western Pacific Ocean clades.

Remarks: *Archinome tethyana* n. sp. is distinguished geographically (Fig. 1), as distinct Clade II (Fig. 3) and by being at least 10% divergent (with COI) from other *Archinome* species.

***Archinome levinae*, new species**

Type Material: HOLOTYPE – SIO-BIC A1365, Costa Rica Mound 11, Costa Rica Margin, 08°55'11"N, 84°18'19"W, 1045 m, 26 February 2009, 1 specimen preserved in 95% Ethanol, *Alvin* Dive 4505 (AT-15), COLL: Greg Rouse, Danwei Huang. PARATYPES – SIO-BIC A1482, Costa Rica Mound 12, Costa Rica Margin, 08°55'47"N, 84°18'48"W, 1008 m, 21 February 2009, 1 specimen preserved in 95% Ethanol, *Alvin* Dive 4501 (AT-15), COLL: Greg Rouse, Danwei Huang; SIO-BIC A1334, Costa Rica Mound 12, Costa Rica Margin, 08°55'42"N, 84°18'47"W, 1000 m, 23 February 2009, 1 specimen preserved in 95% Ethanol, *Alvin* Dive 4502 (AT-15), COLL: Greg Rouse, Danwei Huang; SIO-BIC A1349, Costa Rica Mound 12, Costa Rica Margin, 08°55'50"N, 84°18'25"W, 1005 m, 24 February 2009, 1 specimen preserved in 95% Ethanol, *Alvin* Dive 4503 (AT-15), COLL: Erik Cordes, Jen Gonzalez; SIO-BIC A1398, Costa Rica Mound Quepos, Costa Rica Margin, 09°01'49"N, 84°37'22"W, 1433 m, 26 February 2009, 1 specimen preserved in 95% Ethanol, *Alvin* Dive 4505 (AT-15), COLL: Greg Rouse, Danwei Huang; SIO-BIC A1631, Costa Rica Jaco Scarp, Costa Rica Margin, hydrothermal

seeps, 09°07'00"N, 84°50'06"W, 1817 m, 07 March 2009, 1 specimen preserved in 95% Ethanol, *Alvin* Dive 4513 (AT-15), COLL: Greg Rouse, Danwei Huang; SIO-BIC A2309-A2311, Guaymas Basin, Gulf of California, 27°00'N, 111°24'W, 2432 m, February 2003, 4 specimens preserved in 80% Ethanol, *Tiburon* Dive 551 (Western Flyer), COLL: Robert Vrijenhoek; ADDITIONAL MATERIAL: SIO-BIC A2312 (not included in study), Guaymas Basin, Gulf of California, 27°00'N, 111°24'W, 2432 m, February 2009, 5 specimens preserved in 80% Ethanol, *Tiburon* Dive 551 (Western Flyer), COLL: Robert Vrijenhoek.

Type Locality: 8-9°N, Costa Rica Margin (1008 m)

Diagnosis: Morphology – As described for genus. *Genetics* – Sequences from SIO-BIC A1365 (COI: JX028080; 16S: JX028015; 28S: JX028128; ITS: KF288942) are designated as the genetic diagnoses for *A. levinae* n. sp. Amino acid (AA) *valine* (present in all other *Archinome* species) is substituted for *isoleucine* in COI. Intraspecific range: $d_{\text{COI}} = 0.0\text{--}0.9\%$. Interspecific range: $d_{\text{COI}} = 13.2\text{--}15.9\%$.

Distribution: East Pacific Ocean and Gulf of California. Costa Rican continental margin and Guaymas Basin. Depth range: 1000–2432 m.

Habitat: Hydrothermal vents and cold methane seeps.

Etymology: Named after Professor Lisa Levin (Scripps Institution of Oceanography) for her great contributions to deep-sea exploration and biology and for her love of worms.

Remarks: *Archinome levinae* n. sp. is distinguished from other *Archinome* species geographically (Fig. 1), being supported as distinct Clade III (Fig. 3), by being at least 13% divergent (with COI) from other *Archinome* species and for being the first amphinomid recorded from both vent and seeps. *Archinome levinae* n. sp. is also characterized by the substitution of amino acid *valine* for *isoleucine*, as attributed to a non-synonymous base change of nucleotides

guanine and *adenine*, respectively.

DISCUSSION

Archinome rosacea was originally described as a member of the family Euphrosinidae (Amphinomida) in the genus *Euphrosine* (i.e., *Euphrosine rosacea*). Blake [22] noted affinities to the “fireworm” family Amphinomidae (Amphinomida), but considered them to be “superficial.” Kudenov [11] proposed that the presence of a mixture of morphological characters used to recognize taxa into either amphinomid family (i.e., Amphinomidae and Euphrosinidae) warranted the recognition of a new genus, *Archinome*, and establishment of Archinomidae [11]. Recent molecular phylogenetic work has shown that *Archinome* is a member of Amphinomidae [19, 23], however. The family level status of *Archinome* species is beyond the scope of this study and will be addressed in future work (Borda *et al.*, in preparation). For now, we provide an emended diagnosis of the genus, address the taxonomic statuses of *A. rosacea* and *A. storchi* and describe three new species. In order to provide a framework for unambiguously identifying a suite of *Archinome* species we designated sequenced individuals as type for each of the new species and assigned genetic representatives for *A. rosacea* and *A. storchi*.

With respect to the evaluation of morphology, the absence of consistent diagnosable features attributable to the four species that we consider here was challenged by the topological conflicts among analyses of the concatenated data sets (Fig. 3). Evaluation of ~650 bp of “barcoding COI” supported six distinct clades (Fig. S3A), which were not fully corroborated by 16S, 28S and ITS1 (Fig. S3B-D). Phylogenetic noise owing to COI 3rd codon position saturation is attributed to the observed topological incongruence observed among the combined data analyses, and its inclusion would have led us to an incorrect phylogenetic hypothesis for *Archinome* (Fig. 3B; Fig.

S4B) [24], the latter being mostly driven by the saturated COI signal. However, we accept the presence of *A. rosacea* and *A. storchi* as separate species in the SEPR and a broadly distributed *A. jasoni* found in the Atlantic, Indian and southwest Pacific Oceans, as COI was not saturated below 6% sequence divergence (Fig. S2).

REFERENCES

- 1 Folmer, O., Black, M., Hoeh, W., Lutz, R. & Vrijenhoek, R. 1994 DNA primers for amplification of mitochondrial cytochrome c oxidase subunit I from diverse metazoan invertebrates. *Mol. Mar. Biol. Biotechn.* **3**, 294–299.
- 2 Vrijenhoek, R. C. Cryptic species, phenotypic plasticity, and complex life history: assessing deep-sea fauna diversity with molecular markers. 2009 *Deep-Sea Res. Pt. II*, **56**, 1713–1723. (doi: [10.1016/j.dsr2.2009.05.016](https://doi.org/10.1016/j.dsr2.2009.05.016))
- 3 Siddall, M. E., Fontanella, F. M., Watson, S. C., Kvist, S. & Erséus, C. 2009 Barcoding bamboozled by bacteria: convergence to metazoan mitochondrial primer targets by marine microbes. *Syst Biol* **58**, 445–451.
- 4 Meyer, C. P., Geller, J. B. & Paulay, G. 2005 Fine scale endemism on coral reefs: archipelagic differentiation in turbinid gastropods. *Evolution* **59**, 113–125.
- 5 Edgar, R. C. 2004 MUSCLE: a multiple sequence alignment method with reduced time and space complexity. *BMC Bioinformatics* **5**, 113.
- 6 Edgar, R. C. 2004 MUSCLE: multiple sequence alignment with high accuracy and high throughput. *Nucleic Acids Res* **32**, 1792–1797.
- 7 Maddison, W. P. & Maddison, D. R. 2010 Mesquite: a modular system for evolutionary analysis. Version 2.73 <http://mesquiteproject.org>.
- 8 Posada, D. 2008 jModelTest: phylogenetic model averaging. *Mol. Biol. Evol.* **25**, 1253–1256. (doi: [10.1093/molbev/msn083](https://doi.org/10.1093/molbev/msn083))
- 9 Xia, X. & Xie, Z. 2001 DAMBE: software package for data analysis in molecular biology and evolution. *J. Hered.* **92**, 371–373.

- 10 Tamura, K., Peterson, D., Peterson, N., Stecher, G., Nei, M. & Kumar, S. 2011 MEGA5: molecular evolutionary genetics analysis using maximum likelihood, evolutionary distance, and maximum parsimony methods. *Mol. Biol. Evol.* **28**, 2731–2739. (doi: 10.1093/molbev/msr121)
- 11 Kudenov, J. D. 1991 A new family and genus of the order Amphinomida (Polychaeta) from the Galapagos hydrothermal vents. In: Petersen M. E & Kirkegaard J. B. (eds) Proceedings of the 2nd International Polychaeta Conference, Copenhagen, 1986. Systematics, Biology and Morphology of World Polychaeta. *Ophelia* **5**, 111–120.
- 12 Fiege, D. & Bock, G. 2009 A new species of *Archinome* (Polychaeta: Archinomidae) from hydrothermal vents on the Pacific - Antarctic Ridge 37°S. *J. Mar. Biol. Assoc. U.K.* **89**, 689–696. (doi: <http://dx.doi.org/10.1017/S0025315409000174>)
- 13 Rouse, G. W. & Pleijel, F. 2001 Polychaetes. New York: Oxford University Press.
- 14 Yáñez-Rivera, B. & Carrera-Parra, L. F. 2011 Reestablishment of *Notopygos megalops* McIntosh, description of *N. caribea* sp. n. from the Greater Caribbean and barcoding of “amphiamerican” *Notopygos* species (Annelida, Amphinomidae) *ZooKeys* **223**, 69–84.
- 15 Gustafson, G. 1930 Anatomische studien über die polychäten-familien Amphinomidae und Euphrosynidae. *Zoologiska bidrag från Uppsala*, pp. 305-471.
- 16 Kudenov, J. D. 1995 Family amphinomidae lamarck, 1818. In *Taxonomic atlas of the benthic fauna of the Santa Maria Basin and Western Santa Barbara Channel Vol. 4-7*. (eds J. A. Blake, B. Hilbig & P. H. Scott), pp. 207-215. Santa Barbara: Santa Barbara Museum of Natural History.
- 17 Arhens J., Borda E., Barroso R., Campbell A. M., Wolf A., Nugues M., Paiva P., Rouse G. W. & Schulze A. 2013 The curious case of *Hermodice carunculata* (Annelida:

- Amphinomidae): genetic homogeneity throughout the Atlantic Ocean and adjacent basins. *Mol. Ecol.* **22**, 2280-2291.
- 18 Vogt , J. D. & Kudenov, J. D. 1994 Morphometric variation in the bifurcate notosetae of two *Euphrosine* species. In, Dauvin, J.C., Laubier, L. & Reish, D. J. (eds.), *Actes de la 4eme Conference Internationale des Polychetes. Memoir. Mus. Natl. Natl. Hist.* **162**: 291-298.
- 19 Borda, E., Kudenov, J. D., Beinhold, C. & Rouse, G. W. 2012 Towards a revised Amphinomidae (Annelida: Amphinomida): description and affinities of a new genus and species from the Nile deep-sea Fan, Mediterranean Sea. *Zool. Scri.* **41**, 307–325.
- 20 Ward, M. E., Jenkins, C. D. & Van Dover, C. L. 2003 Functional morphology and feeding strategy of the hydrothermal-vent polychaete *Archinome rosacea* (family Archinomidae). *Can. J. Zool.* **81**, 582–590.
- 21 Shank, T., Fornari, D., Yoerger, D., Humphris, S., Bradley, A., Hammond, S., Lupton, J., Scheirer, D., Collier, R., Reysenbach, A-L. et al. 2003 Deep Submergence Synergy: Alvin and ABE Explore the Galápagos Rift at 86°W *EOS* **84**, 425-440.
- 22 Blake, J. A. 1985 Polychaeta from the vicinity of deep-sea geothermal vents in the eastern Pacific. 1. Euphrosinidae, Phyllodocidae, Hesionidae, Nereidae, Glyceridae, Dorvilleidae, Orbiniidae, and Maldanidae. *Bull. Biol. Soc. Wash.* **6**, 67–101.
- 23 Wiklund, H., Nygren, A., Pleijel, F. & Sundberg, P. 2008 The phylogenetic relationships between Amphinomidae, Archinomidae and Euphrosinidae (Amphinomida: Aciculata: Polychaeta), inferred from molecular data. *J. Mar. Biol. Assoc. U. K.* **88**, 509-513.
- 24 Townsend, J. P., Su, Z. & Tekle, Y. I. 2012 Phylogenetic signal and noise: predicting the power of a data set to resolve phylogeny. *Syst. Biol.* **61**, 835–849.
- (doi:10.1093/sysbio/sys036)

Table S1. Collection locality data, voucher information and GenBank accession numbers for *Archinome* specimens and outgroup taxa included in this study. Species ID based on phylogenetic hypothesis Fig. 3A. Dive # vehicle designation: A=HOV *Alvin* (WHOI); T=ROV *Tiburon* (MBARI); N=HOV *Nautilite* (IFREMER); V=ROV *Victor 6000* (IFREMER); J1=ROV *Jason* (WHOI); J2= ROV *Jason II* (WHOI); HOV=Human occupied vehicle; ROV=remote operated vehicle. Habitat type designation for each locality: V=vent; S=seep.

LOCALITY	SPECIES ID	DIVE #	COORDINATES	DEPTH (M)	VOUCHER ID	COI	16S	28S	ITS1
Galapagos Rift									
Rose Bud (V)	<i>A. rosacea</i>	A4115	00°48'N, 86°13'W	2451	WHOI 4115-3-1	JX028057	JX027992	--	KF288954
Rose Bud (V)	<i>A. rosacea</i>	A4115	00°48'N, 86°13'W	2451	WHOI 4115-3-2	JX028058	JX027993	JX028121	--
Rose Bud (V)	<i>A. rosacea</i>	A4115	00°48'N, 86°13'W	2451	WHOI 4115-3-3	JX028059	JX027994	JX028122	KF288955
Rose Bud (V)	<i>A. rosacea</i>	A4115	00°48'N, 86°13'W	2451	WHOI 4115-3-4	JX028060	JX027995	--	KF288956
Rose Bud (V)	<i>A. rosacea</i>	A4115	00°48'N, 86°13'W	2451	WHOI 4115-3-5	JX028061	JX027996	--	KF288957
Rose Bud (V)	<i>A. rosacea</i>	A4115	00°48'N, 86°13'W	2451	WHOI 4115-3-6	JX028062	JX027997	--	--
Galapagos Rift (V)	<i>A. rosacea</i>	A2223	00°48'N, 86°09'W	2515	--	JX028108	JX028043	--	--
Pacific Antarctic Ridge									
37°S (V)	<i>A. storchi</i>	A4088	37°47'N, 110°54'W	2216	SIO-BIC A2316	JX028065	JX028000	--	KF288936
37°S (V)	<i>A. storchi</i>	A4088	37°47'N, 110°54'W	2216	SIO-BIC A2317	JX028066	JX028001	--	--
37°S (V)	<i>A. storchi</i>	A4090	37°47'N, 110°54'W	2220	SIO-BIC A2318	JX028067	JX028002	JX028125	KF288937
North East Pacific Rise									
Guaymas Basin (V)	<i>A. levinae</i>	T551	27°00'N, 111°24'W	2432	SIO-BIC A2309	JX028063	JX027998	JX028123	--
Guaymas Basin (V)	<i>A. levinae</i>	T551	27°00'N, 111°24'W	2432	SIO-BIC A2310	JX028101	JX028036	JX028134	--
Guaymas Basin (V)	<i>A. levinae</i>	T551	27°00'N, 111°24'W	2432	SIO-BIC A2311	JX028102	JX028037	--	--
9°N (V)	<i>A. rosacea</i>	A3763	9°46'N, 104°16'W	2505	SIO-BIC A2875	JX028109	JX028044	--	--
9°N (V)	<i>A. rosacea</i>	A3763	9°46'N, 104°16'W	2505	SIO-BIC A2876	JX028110	JX028045	--	--
9°N (V)	<i>A. rosacea</i>	A3763	9°46'N, 104°16'W	2505	SIO-BIC A2877	JX028111	JX028046	--	--
9°N (V)	<i>A. rosacea</i>	N1738	9°47'N, 104°16'W	2515	SIO-BIC A2881	JX028105	JX028040	JX028137	--
9°N (V)	<i>A. rosacea</i>	N1738	9°47'N, 104°16'W	2515	SIO-BIC A2882	JX028106	JX028041	--	--
9°N (V)	<i>A. rosacea</i>	N1742	9°47'N, 104°16'W	2515	SIO-BIC A2883	JX028107	JX028042	JX028138	--
South East Pacific Rise									
7°S (V)	<i>A. rosacea</i>	N1572	07°24'S, 107°47'W	2746	SIO-BIC A2890	JX028083	JX028018	--	--
7°S (V)	<i>A. rosacea</i>	N1571	07°22'S, 107°47'W	2719	SIO-BIC A2891	JX028084	JX028019	JX028129	KF288943
7°S (V)	<i>A. rosacea</i>	N1573	07°25'S, 107°47'W	2750	SIO-BIC A2892	JX028085	JX028020	--	--
17°S (V)	<i>A. storchi</i>	N1590	17°25'S, 113°12'W	2585	SIO-BIC A2389	JN086543	JN086552	JN086523	--
18°S (V)	<i>A. storchi</i>	N1585	18°36'S, 113°24'W	2680	--	JX028086	JX028021	JX028130	--
18°S (V)	<i>A. storchi</i>	N1585	18°36'S, 113°24'W	2680	--	JX028087	JX028022	--	KF288944
18°S (V)	<i>A. storchi</i>	N1585	18°36'S, 113°24'W	2680	--	JX028088	JX028023	--	--
21°S (V)	<i>A. storchi</i>	N1577	21°33'S, 114°17'W	2838	--	JX028089	JX028024	--	--
21°S (V)	<i>A. storchi</i>	N1577	21°33'S, 114°17'W	2838	--	JX028090	JX028025	--	KF288945
21°S (V)	<i>A. storchi</i>	N1577	21°33'S, 114°17'W	2838	--	JX028091	JX028026	--	--
23°S (V)	<i>A. storchi</i>	A4096	23°32'S, 115°34'W	2595	SIO-BIC A2353	JX028074	JX028009	--	KF288940
23°S (V)	<i>A. storchi</i>	A4096	23°32'S, 115°34'W	2595	SIO-BIC A2354	JX028075	JX028010	--	--

Table S1 (CONT'D)										
LOCALITY	SPECIES	DIVE #	COORDINATES	DEPTH (M)	VOUCHER ID	COI	16S	28S	ITS1	
South East Pacific Rise										
23°S (V)	<i>A. storchi</i>	A4096	23°32'S, 115°34'W	2595	--	JX028076	JX028011	JX028126	--	
31°S (V)	<i>A. storchi</i>	A4092	31°51'S, 112°02'W	2334	SIO-BIC A2355	JX028068	JX028003	--	--	
31°S (V)	<i>A. storchi</i>	A4092	31°51'S, 112°02'W	2334	SIO-BIC A2356	JX028069	JX028004	--	--	
31°S (V)	<i>A. storchi</i>	A4092	31°51'S, 112°02'W	2334	SIO-BIC A2357	JX028070	JX028005	--	--	
31°S (V)	<i>A. storchi</i>	A4094	31°00'S, 111°55'W	2334	SIO-BIC A2359	JX028071	JX028006	--	KF288938	
31°S (V)	<i>A. storchi</i>	A4094	31°00'S, 111°55'W	2337	SIO-BIC A2360	JX028072	JX028007	--	--	
31°S (V)	<i>A. storchi</i>	A4094	31°00'S, 111°55'W	2337	SIO-BIC A2361	JX028073	JX028008	--	KF288939	
Costa Rica Margin										
8°N (S)	<i>A. levinae</i>	A4501	08°55'N, 84°18'W	1008	SIO-BIC A1482	JX028077	JX028012	JX028127	--	
8°N (S)	<i>A. levinae</i>	A4502	08°55'N, 84°18'W	1000	SIO-BIC A1334	JX028078	JX028013	--	--	
8°N (S)	<i>A. levinae</i>	A4503	08°55'N, 84°18'W	1005	SIO-BIC A1349	JX028079	JX028014	--	KF288941	
8°N (S)	<i>A. levinae</i>	A4505	08°55'N, 84°18'W	1045	SIO-BIC A1365	JX028080	JX028015	JX028128	KF288942	
9°N (S)	<i>A. levinae</i>	A4508	09°01'N, 84°37'W	1433	SIO-BIC A1398	JX028081	JX028016	--	--	
9°N (HS)	<i>A. levinae</i>	A4513	09°07'N, 84°50'W	1817	SIO-BIC A1631	JX028082	JX028017	--	--	
Mid Atlantic Ridge										
Broken Spur (V)	<i>A. tethyana</i>	A3124	29°10'N, 43°10'W	3056	--	--	JX028047	--	--	
TAG (V)	<i>A. tethyana</i>	A3126	26°08'N, 44°49'W	3655	--	--	JX028048	--	--	
Snake Pit (V)	<i>A. tethyana</i>	A3128	23°22'N, 44°56'W	3660	--	--	JX028049	--	--	
Logatchev (V)	<i>A. jasoni</i>	A3133	14°45'N, 44°58'W	3038	--	JX028112	JX028050	--	--	
Logatchev (V)	<i>A. jasoni</i>	A3133	14°45'N, 44°58'W	3038	--	--	JX028051	--	--	
Ashadze-1 (V)	<i>A. tethyana</i>	V312	12°58'N, 44°51'W	4080	SIO-BIC A2871	--	JX028052	--	KF288958	
Ashadze-1 (V)	<i>A. tethyana</i>	V312	12°58'N, 44°51'W	4080	SIO-BIC A2872	--	JX028053	--	KF288959	
Ashadze-1 (V)	<i>A. tethyana</i>	V312	12°58'N, 44°51'W	4080	SIO-BIC A2873	JX028113	JX028054	JX028139	--	
Ashadze-1 (V)	<i>A. tethyana</i>	V312	12°58'N, 44°51'W	4080	SIO-BIC A2874	JX028114	JX028055	JX028140	--	
Central India Ridge										
Kairei Field (V)	<i>A. jasoni</i>	J1S297	25°19'S, 70°02'E	2432	SIO-BIC A2313	JX028064	JX027999	JX028124	KF288935	
Kairei Field (V)	<i>A. jasoni</i>	J1S297	25°19'S, 70°02'E	2432	SIO-BIC A2314	JX028103	JX028038	JX028135	--	
Kairei Field (V)	<i>A. jasoni</i>	J1S297	25°19'S, 70°02'E	2432	SIO-BIC A2315	JX028104	JX028039	JX028136	KF288953	
Southwest Pacific Basins										
North Fiji (V)	<i>A. jasoni</i>	J2-149	16°59'S, 173°54'E	1985	SIO-BIC A2365	JX028098	JX028033	--	KF288952	
North Fiji (V)	<i>A. jasoni</i>	J2-149	16°59'S, 173°54'E	1985	SIO-BIC A2366	JX028099	JX028034	--	--	
North Fiji (V)	<i>A. jasoni</i>	J2-149	16°59'S, 173°54'E	1985	SIO-BIC A2367	JX028100	JX028035	JX028133	--	
Kilo Moana (V)	<i>A. jasoni</i>	J2-140	20°59'S, 176°08'E	2650	SIO-BIC A2369	JX028095	JX028030	--	KF288949	
Kilo Moana (V)	<i>A. jasoni</i>	J2-140	20°59'S, 176°08'E	2650	SIO-BIC A2370	JX028096	JX028031	--	KF288950	
Kilo Moana (V)	<i>A. jasoni</i>	J2-140	20°59'S, 176°08'E	2650	SIO-BIC A2371	JX028097	JX028032	--	KF288951	

Table S1 (CONT'D)									
LOCALITY	SPECIES	DIVE #	COORDINATES	DEPTH (M)	VOUCHER ID	COI	16S	28S	ITS1
Tui Malila Lau (V)	<i>A. jasoni</i>	J2-144	21°59'S, 176°34'E	1900	SIO-BIC A2375	JX028092	JX028027	JX028131	KF288946
Tui Malila Lau (V)	<i>A. jasoni</i>	J2-144	21°59'S, 176°34'E	1900	SIO-BIC A2376	JX028093	JX028028	--	KF288947
Tui Malila Lau (V)	<i>A. jasoni</i>	J2-144	21°59'S, 176°34'E	1900	SIO-BIC A2377	JX028094	JX028029	JX028132	KF288948
OUTGROUP	LOCALITY		COORDINATES	DEPTH (M)	VOUCHER ID	COI	16S	28S	
<i>Chloeia viridis</i>	Florida, USA		24°27'N, 83°11'W	n/a	UF Annelida 478	JN086546	JN086555	JN086527	
<i>Notopygos ornata</i>	Acapulco, Mexico		16°51'N, 99°54'W	n/a	ECO-OH-P0223	JX028115	JX028056	JX028141	

1

2

3

Table S2. Primers used for COI and 16S amplification and sequencing reactions.

PRIMER	SEQUENCE5'-3'	REFERENCE
16S		
arL	CGCCTGTTTATCAAAAACAT	Palumbi et al., 1991
brH	CCGGTCTGAACTCAGATCACGT	Palumbi et al., 1991
AnnF	GCGGTATCCTGACCGTRCWAAGGTA	Sjölin et al. (2005)
AnnR	TCCTAAGCCAACATCGAGGTGCCAA	Sjölin et al. (2005)
COI		
dgLCO	GGTCAACAAATCATAAAGAYATYGG	Meyer et al. (2005)
dgHCO	TAAACTTCAGGGTGACCAAARAAYCA	Meyer et al. (2005)
AROCOI2F	AAGACATCGGCACCCTATACCTCA	This study
AROCOI559R	AGAGGTGTTTAGGTTCCGGTCTGT	This study

16S: 94°C (3m); 5 cycles: 94°C (30m), 46°C (30m), 72°C (45s); 30 cycles: 94°C (30m), 50°C (30m), 72°C (45s); 72°C (7m)

COI: 94°C (3m); 30 cycles: 94°C (1m), 52°C (1m), 72°C (45s); 72°C (7m)

Table S3. Mean TrN corrected (below diagonal) and uncorrected (above diagonal) pairwise distances for COI (italics) and ITS1 (bold italics) among select *Archinome* populations. Roman numerals reflect *Archinome* clades on Figure 3. CIR=Central Indian Ridge; SWP=Southwest Pacific Basins; LOG=Logatchev; A1=Ashadze-1; GB=Guaymas Basin; CRM=Costa Rica Margin; GAR=Galapagos Rift; NEPR=North East Pacific Rise; SEPR=South East Pacific Rise.

	I CIR (25°N)	I SWP (16-20°S)	I LOG (14°N)	II A1 (12°N)	III GB (27°N)	III CRM (8-9°N)	IV GAR (0°N)	IV NEPR (9°N)	IV SEPR1 (7°S)	V SEPR2 (17-18°S)	V SEPR3 (37°S)
CIR	*	0.029 0.001	0.003 --	0.100 0.013	0.133 --	0.132 0.019	0.136 0.012	0.136 --	0.134 0.013	0.133 0.013	0.133 0.013
SWP	0.030 0.001	*	0.032 --	0.109 0.014	0.132 --	0.134 0.020	0.148 0.013	0.148 --	0.147 0.014	0.141 0.014	0.141 0.014
LOG	0.003 --	0.034 --	*	0.101 --	0.135 --	0.134 --	0.137 --	0.137 --	0.136 --	0.134 --	0.134 --
A1	0.110 --	0.121 0.014	0.112 --	*	0.130 --	0.129 0.032	0.112 0.025	0.112 --	0.111 0.025	0.113 0.025	0.111 0.025
GB	0.149 --	0.148 --	0.152 --	0.146 --	*	0.004 --	0.126 --	0.126 --	0.126 --	0.130 --	0.131 --
CRM	0.149 0.019	0.151 0.020	0.151 --	0.145 0.033	0.004 --	*	0.124 0.031	0.124 --	0.124 0.032	0.129 0.032	0.130 0.032
GAR	0.157 0.012	0.173 0.013	0.159 --	0.125 0.025	0.141 --	0.139 0.032	*	0.005 --	0.008 0.004	0.047 0.004	0.047 0.004
NEPR	0.157 --	0.173 --	0.159 --	0.125 --	0.141 --	0.139 --	0.005 --	*	0.008 --	0.047 --	0.046 --
SEPR1	0.155 0.013	0.171 0.014	0.157 --	0.123 0.026	0.141 --	0.139 0.033	0.008 0.004	0.008 --	*	0.047 0.006	0.046 0.006
SEPR2	0.154 0.013	0.164 0.014	0.155 --	0.125 0.026	0.147 --	0.145 0.033	0.050 0.004	0.049 --	0.049 0.006	*	0.003 0.000
SEPR3	0.154 0.013	0.164 0.014	0.155 --	0.124 0.026	0.148 --	0.146 0.033	0.049 0.004	0.048 --	0.048 0.006	0.003 0.000	*

I. *A. jasoni* n. sp. II. *A. tethyana* n. sp. III. *A. levinae* n. sp. IV. *A. rosacea* V. *A. storchi*

Table S4. Summary of morphological characters evaluated among *Archinome* species.

1. Number of chaetigers
2. Length (mm), excluding prostomial appendages
3. Width (mm), excluding chaetae
4. Body shape
5. Body shape, cross section, mid section
6. Median antenna, shape (homologous to nuchal cirrus, *sensu* Fiege and Bock, 2009)
7. Median antenna, length (l) to width (w) ratio: a) minute, <2x; b) short, 2–3x; c) long, >6x
8. Antennae, shape (homologous to dorsomedial antennae, *sensu* Fiege and Bock, 2009)
9. Antennae, length (l) to width (w) ratio: a) short, >6x; b) moderate, 6–8x; c) long, >9x
10. Antennae, extending laterally to: a) prostomial margins; b) notopodium, chaetiger 1; c) notopodium chaetiger 2
11. Palps, shape
12. Palps, length relative to antennae
13. Palps, length (l) to width (w) ratio
14. Palps, extending laterally to neuropodium chaetiger 1
15. Mouth, opening between chaetigers 2–3
16. Midventral muscular scutes
17. Midventral muscular scutes fused anteriorly, from chaetiger 2 through chaetigers (number).
Note: Scutes normally separated by well-defined segmental annuli in small specimens, fused into large plates that are either partially (denoted by /) or completely (denoted by -) lacking segmental annuli in larger specimens.
18. Eyespots, 1 pair dorsal and 1 pair ventral on prostomium
19. Caruncle, shape
20. Caruncle, extending to chaetiger (number)
21. Caruncle, position within chaetiger from 20: a) anterior margin; b) mid-chaetiger; c) posterior margin
22. Caruncle, fixed to body wall through chaetiger 2; b) through chaetiger 4, overlapping chaetiger 5
23. Caruncle, free of body wall: a) chaetigers 3; b) chaetigers 3–4; c) chaetigers 3–5
24. Chaetiger 1, size
25. Parapodia, type
26. Notopodia, shape
27. Notopodia, shape
28. Neuropodia, shape
29. Neuropodia, shape
30. Dorsal cirri
31. Dorsal cirriphore
32. Ventral cirri
33. Dorsal accessory cirri
34. Branchia (type)
35. Branchia, first chaetiger appearance
36. Branchia, number of filaments
37. Branchia, maximum number of filaments
38. Chaetae, overall features

39. Notochaetae, type
40. Notochaetae, long:short prong ratio. Prongs measured from distal tip of each prong to inner chaetal junction from where tines diverge from one another (Vogt & Kudenov 1994).
41. Notochaetae, prong angle, degrees. Angle measured between distal tips of each prong to inner chaetal junction from where tines diverge from one another.
42. Notochaetae, area $\mu\text{m}^2 \times 10^3$. Measured prong lengths and angles used to calculate area (μm^2) of triangle formed using the formula $\text{Area} = (A^2+B^2-2AB\cos(C))^{1/2}$ where A and B represent lengths of long and short prongs, and C is the angle in radians.
43. Notochaetae, asperites. Taxonomic term describing variously developed minute file-like points or denticles on surface of chaetal shafts proximal to distal prongs.
44. Notochaetae, spurred
45. Neurochaetae, type
46. Neurochaetae, long:short prong ratio. Prongs measured from distal tip of each prong to inner chaetal junction from where tines diverge from one another (Vogt & Kudenov 1994).
47. Neurochaetae, prong angle, degrees. Angle measured between distal tips of each prong to inner chaetal junction from where tines diverge from one another.
48. Neurochaetae, area $\mu\text{m}^2 \times 10^3$. Measured prong lengths and angles used to calculate area (μm^2) of triangle formed using the formula $\text{Area} = (A^2+B^2-2AB\cos(C))^{1/2}$ where A and B represent lengths of long and short prongs, and C is the angle in radians.
49. Neurochaetae, asperites. Taxonomic term describing variously developed minute file-like points or denticles on surface of chaetal shafts proximal to distal prongs.
50. Neuroacicula, spurred
51. Pygidial, cirrus
52. Anus, dorsal opening on segments
53. Anus, extending through segments
54. Pygidial "eyespot": (0) 1 pair of lateral stripes, terminally absent; (1) transverse distal band, terminal; (2) distal patch, terminal; (3) middorsal patch, base to tip; (4) absent

Table S5. Comparison of morphological characters (Table S4) among select *Archinome* specimens. **Holotype

	<i>A. rosacea</i> **	<i>A. rosacea</i>	<i>A. rosacea</i>	<i>A. storchi</i>	<i>A. storchi</i> **	<i>A. jasoni n. sp.</i>	<i>A. tethyana n. sp.</i>	<i>A. levinae n. sp.</i>			
	GAR (0°N)	NEPR (9°N)	GAR (0°N)	SEPR (17°S)	PAR (37°S)	CIR (25°S)	MAR (14°N)	SWP (22°S)	SWP (22°S)	MAR (23°N)	CRM (9°N)
1	18	23	10	11	23	32	24	20	18	33	23
2	12 mm	14 mm	1.2 mm	1.2 mm	15 mm	27 mm	9 mm	8 mm	7 mm	38 mm	14 mm
3	5.5 mm	5.5 mm	0.8 mm	1 mm	4.5 mm	10.5 mm	3 mm	2.5 mm	2.5 mm	7 mm	6 mm
4	Fusiform										
5	Trapezoidal										
6	Cirriform	Cirriform	Conical	Cirriform	Cirriform	Cirriform	Papilliform	Cirriform	Claviform	Cirriform	
7	Short	Short	Short	Short	Long	Minute	Minute	Short	Short	Minute	Minute
8	Cirriform										
9	Short	Short	Short	Short	Long	Moderate	Moderate	Long	Moderate	Short	Moderate
10	Prost. margin	Noto. ch. 1	Noto. ch. 1	Noto. ch. 1	Noto. ch. 1	Noto. ch. 1-2	Noto. ch. 1-2	Noto. ch. 1-2	Noto. ch. 1-2	Noto. ch. 2	Noto. ch. 2
11	Cirriform										
12	As long	As long	Longer	Longer	Shorter	Shorter	Shorter	Shorter	Shorter	Shorter	As long
13	6.3x	6.4x	5.5x	5.2	6.6-7x	5.5x	3.1x	7.6x	7.5x	3.6x	6.5x
14	1										
15	2-3										
16	Present										
17	2-3	2-3/4	2-3	2-3	2-3	2-4	2-5	2-4	2-4	2-5	2-3
18	1 pair dorsal, 1 pair ventral										
19	Elongate, trilobed										
20	5	4	3	3	4	3	3	3	5	4	3
21	Ant. mar.	Ant. mar.	Mid. chaet	Mid. chaet	Mid. chaet	Post. mar.	Mid. chaet.	Post. mar.	Ant. mar.	Mid. chaet.	Post. mar.

Table S5. (cont'd)

	<i>A. rosacea</i> **	<i>A. rosacea</i>	<i>A. rosacea</i>	<i>A. storchi</i>	<i>A. storchi</i> **	<i>A. jasoni n. sp.</i>	<i>A. jasoni n. sp.</i>	<i>A. jasoni n. sp.</i>	<i>A. jasoni n. sp.</i>	<i>A. tethyana n. sp.</i>	<i>A. levinae n. sp.</i>
	GAR (0°N)	NEPR (9°N)	GAR (0°N)	SEPR (17°S)	PAR (37°S)	CIR (25°S)	MAR (14°N)	SWP (22°S)	SWP (22°S)	MAR (23°N)	CRM (9°N)
22						2					
23	3-5	3-4	3	3	3-4	3	3	3	3-5	3-4	
24	Reduced	Reduced	Reduced	Reduced	Reduced	Reduced	Enlarged	Enlarged	Enlarged	Reduced	Reduced
25						Biramous					
26						Conical					
27						Circular					
28						Mound-shaped					
29						Circular					
30						Present					
31						Present					
32						Present					
33						Present					
34						Digitiform					
35						3					
36	1-2	3	1	1	3	5	2	3	3	4	3
37	6	7-8	1	1	7	15-16	4	5	5	7-9	>15
38						Simple, calcareous, brittle					
39						Bifurcate					
40	5.3-10.7:1	3.8-6.3:1	7.4-10.4	2.8-5.2:1	2.7-5.2:1	4.8-8.7:1	4.2-7.6:1	4.3-5.9:1	3.2-5.2:1	3-6:1	4.25:1
41	23.2	22.9	26.9	22.9	23.3	32.4	28.3	31.2	30.5	21.6	22.5
42	7.7	7.4	0.6	1.7	2	4.2	2.1	4.1	12	2.6	7.1
43						Present					

Table S5. (cont'd)

	<i>A. rosacea</i> **	<i>A. rosacea</i>	<i>A. rosacea</i>	<i>A. storchi</i>	<i>A. storchi</i> **	<i>A. jasoni n. sp.</i>	<i>A. tethyana n. sp.</i>	<i>A. levinae n. sp.</i>			
	GAR1 (0°N)	NEPR (9°N)	GAR2 (0°N)	SEPR (17°S)	PAR (37°S)	CIR (25°S)	MAR1 (14°N)	SWP1 (22°S)	SWP2 (22°S)	MAR2 (23°N)	CRM (9°N)
44						Present					
45						Bifurcate					
46	2.1-4.7:1	2.3-4.6:1	9.3-17.8	2.7-4.6:1	2.7-4.6:1	3.2-5:1	2.5-5.8:1	3.4-6.1:1	1.6-2.7	2-5.1:1	2.3-5.1:1
47	22.6	20.8	38	22.7	22.7	25.2	20.3	30.9	21.5	17.4	n/a
48	2.7	5.2	0.26	1.6	1.6	5.4	3.5	3	4.9	2.4	n/a
49						Present					
50						Present					
51						Thick, elongate					
52	17-18	18-20	9	10	19-20	22-26	21-23	18-19	16-17	25-27	19-20
53	2	2-3	1	1	2	2-4	2-3	2	2	2-3	2
54	0	0	4	4	0	1	2	4	4	3	0

A. rosacea (GAR1) USNM 81788, Holotype
A. rosacea (NEPR) SIO-BIC A3542
A. rosacea (GAR2) USNM 1221442
A. storchi (SEPR) SIO-BIC A3543
A. storchi (PAR) SMF 17876, Holotype
A. jasoni n. sp. (CIR) SIO-BIC A3544

A. jasoni n. sp. (MAR) SIO-BIC A3545
A. jasoni n. sp. (SWP) SIO-BIC A3546
A. jasoni n. sp. (SWP) SIO-BIC A3547
A. tethyana n. sp. (MAR) SIO-BIC A3548
A. levinae n. sp. (CRM) SIO-BIC A1316

1 **ESM FIGURE LEGENDS**

2

3 **Figure S1.** General aspects of *Archinome* morphology and main diagnostic characters. A. Doral
4 view of anterior-most body segments. B. Ventral view of diagnostic characters. a=antenna;
5 b=branchia; bc=bifurcate chaetae; bci=dorsal accessory cirrus; c=chaetae; ca=caruncle;
6 dc=dorsal cirrus; des=dorsal eyespot; ma=median antenna; mvs=midventral scute; p=palps;
7 pc=pygidial cirrus; vc=ventral cirrus; ves=ventral eyespot

8

9 **Figure S2.** Saturation plot of transitions (s) and transversions (v) of all three codon positions
10 (all) and third codon position alone (3rd) against the TrN corrected genetic distances of
11 *Archinome* COI sequences.

12

13 **Figure S3.** Phylogenetic hypotheses of *Archinome* (BI topology shown) based on single gene
14 analyses. A. COI_{ALL}; B. 16S; C. 28S; D. ITS1. ML bootstrap and BI posterior probabilities
15 (boot/pp) shown at nodes; * denote boot >90% and pp >0.95; values below 80% not shown.

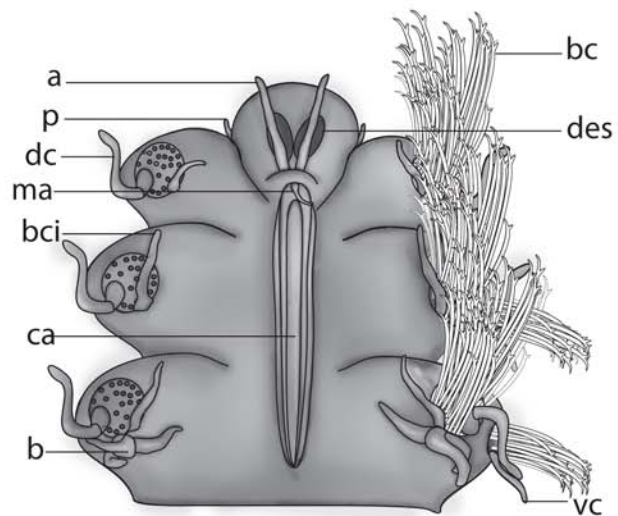
16

17 **Figure S4.** Phylogenetic hypotheses of *Archinome* (ML topology shown) based on COI and 16S.
18 A. COI_{NO3RD}+16S; B. COI_{ALL}+16S. ML bootstrap and BI posterior probabilities (boot/pp) shown
19 at nodes; * denote boot >90% and pp >0.95; values below 80% not shown.

20

Figure S1

A.



B.

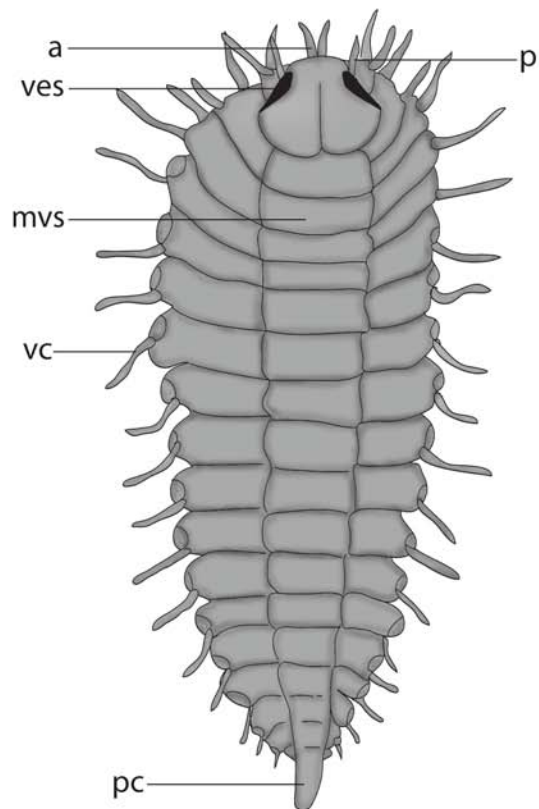


Figure S2

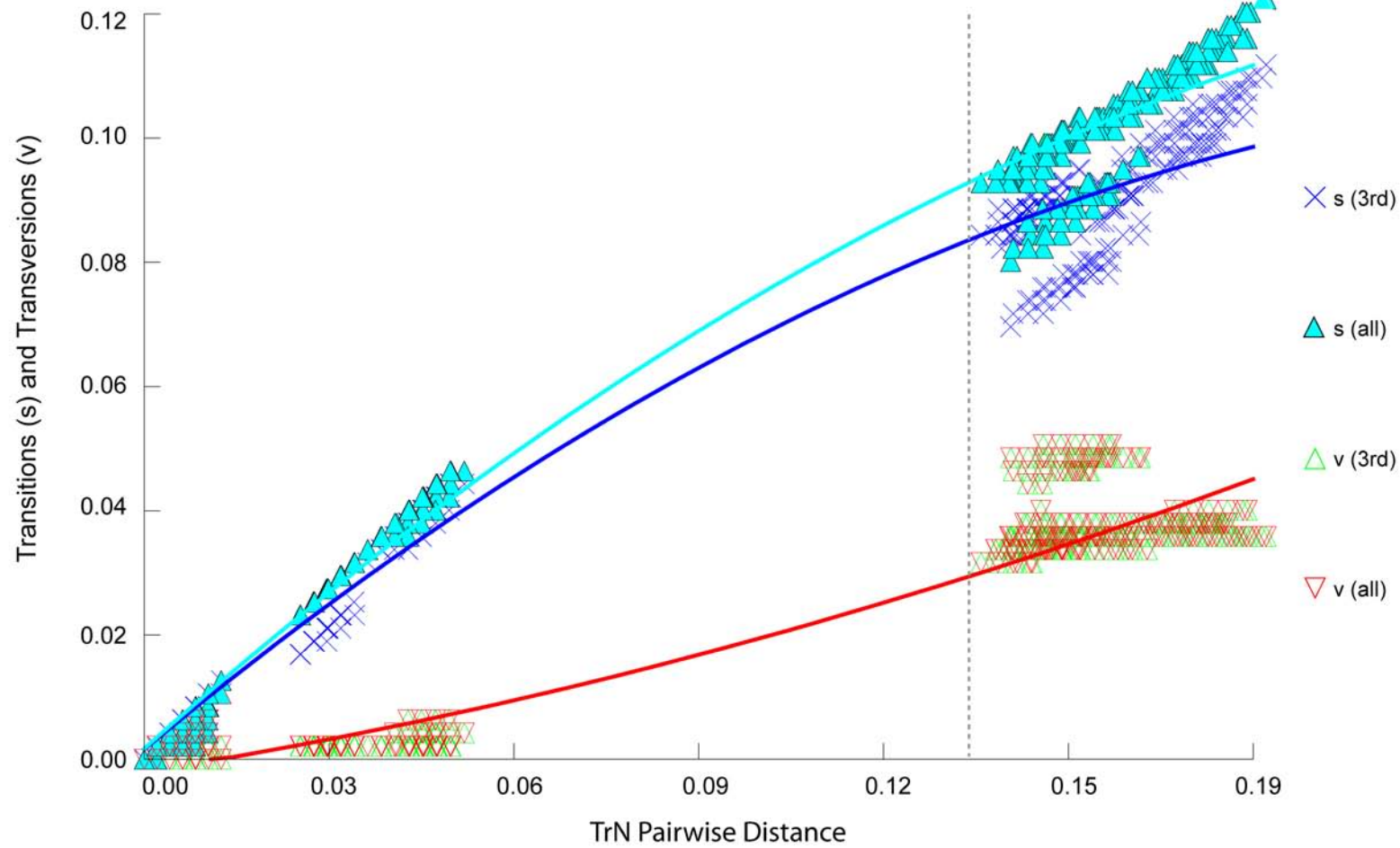
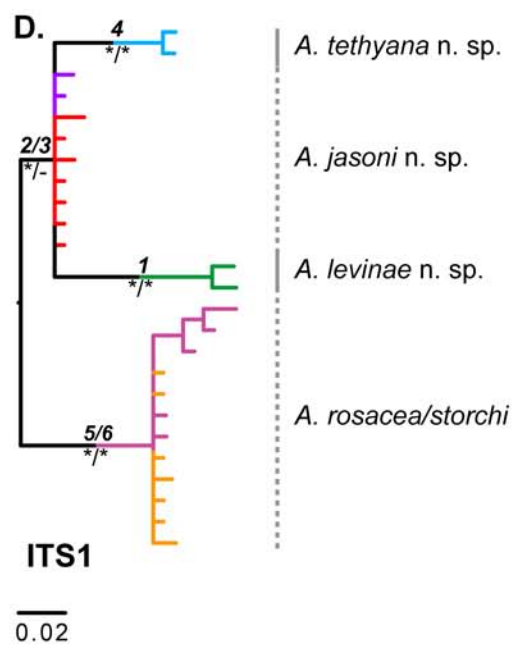
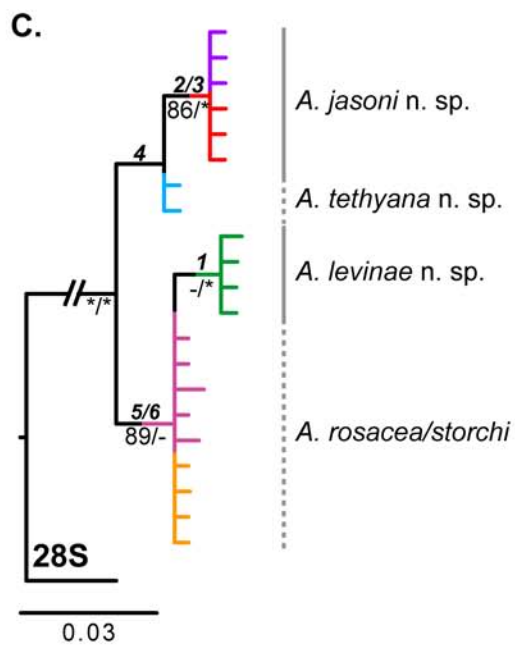
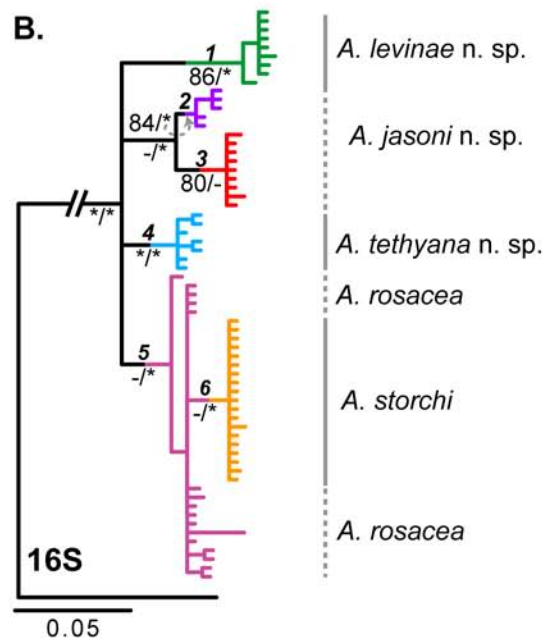
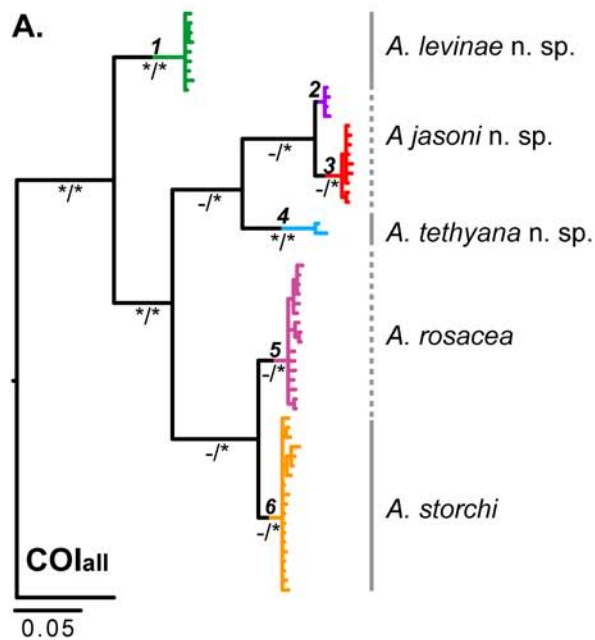
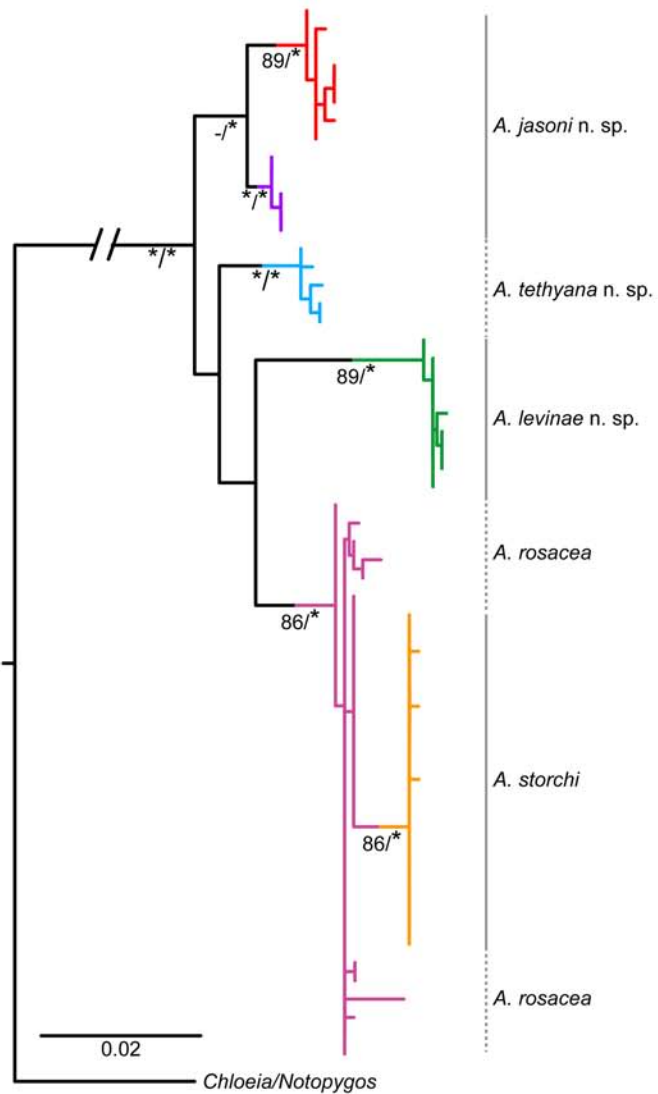


Figure S3



A.



B.

